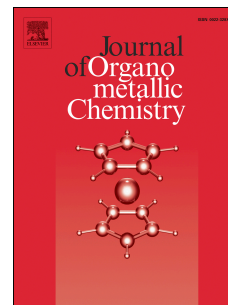


# Journal Pre-proof

Synthesis, structural and electrochemical characterization of novel ferrocene-containing tetrahydropyrimidin-2(1*H*)-ones

Aleksandra Minić, Marko S. Pešić, Sladjana B. Novaković, Goran A. Bogdanović, Anka Todosijević, Danijela Ilić Komatina, Dragana Stevanović



PII: S0022-328X(20)30324-7

DOI: <https://doi.org/10.1016/j.jorganchem.2020.121422>

Reference: JOM 121422

To appear in: *Journal of Organometallic Chemistry*

Received Date: 3 June 2020

Revised Date: 28 June 2020

Accepted Date: 5 July 2020

Please cite this article as: A. Minić, M.S. Pešić, S.B. Novaković, G.A. Bogdanović, A. Todosijević, Danijela Ilić Komatina, D. Stevanović, Synthesis, structural and electrochemical characterization of novel ferrocene-containing tetrahydropyrimidin-2(1*H*)-ones, *Journal of Organometallic Chemistry* (2020), doi: <https://doi.org/10.1016/j.jorganchem.2020.121422>.

This is a PDF file of an article that has undergone enhancements after acceptance, such as the addition of a cover page and metadata, and formatting for readability, but it is not yet the definitive version of record. This version will undergo additional copyediting, typesetting and review before it is published in its final form, but we are providing this version to give early visibility of the article. Please note that, during the production process, errors may be discovered which could affect the content, and all legal disclaimers that apply to the journal pertain.

© 2020 Published by Elsevier B.V.

# Synthesis, structural and electrochemical characterization of novel ferrocene-containing tetrahydropyrimidin-2(1*H*)-ones

Aleksandra Minić,<sup>\*a</sup> Marko S. Pešić,<sup>b</sup> Sladjana B. Novaković,<sup>c</sup> Goran A. Bogdanović,<sup>c</sup> Anka Todosijević,<sup>d</sup> Danijela Ilić Komatina,<sup>a</sup> Dragana Stevanović<sup>b</sup>

<sup>a</sup>Faculty of Technical Sciences, University of Priština, Knjaza Miloša 7, 38220 Kosovska Mitrovica, Serbia

<sup>b</sup>Department of Chemistry, Faculty of Science, University of Kragujevac, Radoja Domanovića 12, 34000 Kragujevac, Serbia

<sup>c</sup>„VINČA” Institute of Nuclear Sciences - National Institute of the Republic of Serbia, University of Belgrade, PO Box 522, 11001 Belgrade, Serbia

<sup>d</sup>Faculty of Agriculture, University of Niš, Kosančićeva 4, 37000 Kruševac, Serbia

\*Corresponding author: [aleksandra.minic.989@gmail.com](mailto:aleksandra.minic.989@gmail.com) ([aleksandra.minic@pr.ac.rs](mailto:aleksandra.minic@pr.ac.rs))

**Abstract:** Herein, we report an easy performable method for the synthesis of ferrocene-containing tetrahydropyrimidin-2(1*H*)-ones starting from the corresponding 3-arylamino-1-ferrocenylpropan-1-ols and sodium cyanate (NaOCN) in the presence of glacial acetic acid. The protocol is included an intramolecular cyclization of an *in situ* generated 1,3-hydroxyurea. The scope of the reaction towards eleven ferrocene-containing 1,3-amino alcohols has been explored and the targeted 1-aryl-4-ferrocenyltetrahydropyrimidin-2(1*H*)-ones were obtained in good to high yields (up to 93%). All products have been isolated in high purity >95%. In addition, we have provided a detailed structural characterization of the new compounds, which has been performed by IR and NMR spectroscopy. The single-crystal X-ray diffraction analysis was successfully performed on three representative examples, as well as elemental analysis. Moreover, molecular structure properties and intermolecular interactions of these three structures have been compared and analyzed in detail. Electrochemical properties of products were investigated by cyclic voltammetry. This investigation revealed the quasi-reversible one-electron redox process.

**Keywords:** Ferrocene, Tetrahydropyrimidin-2(1*H*)-ones, One-pot reaction, Crystal structure, Electrochemistry.

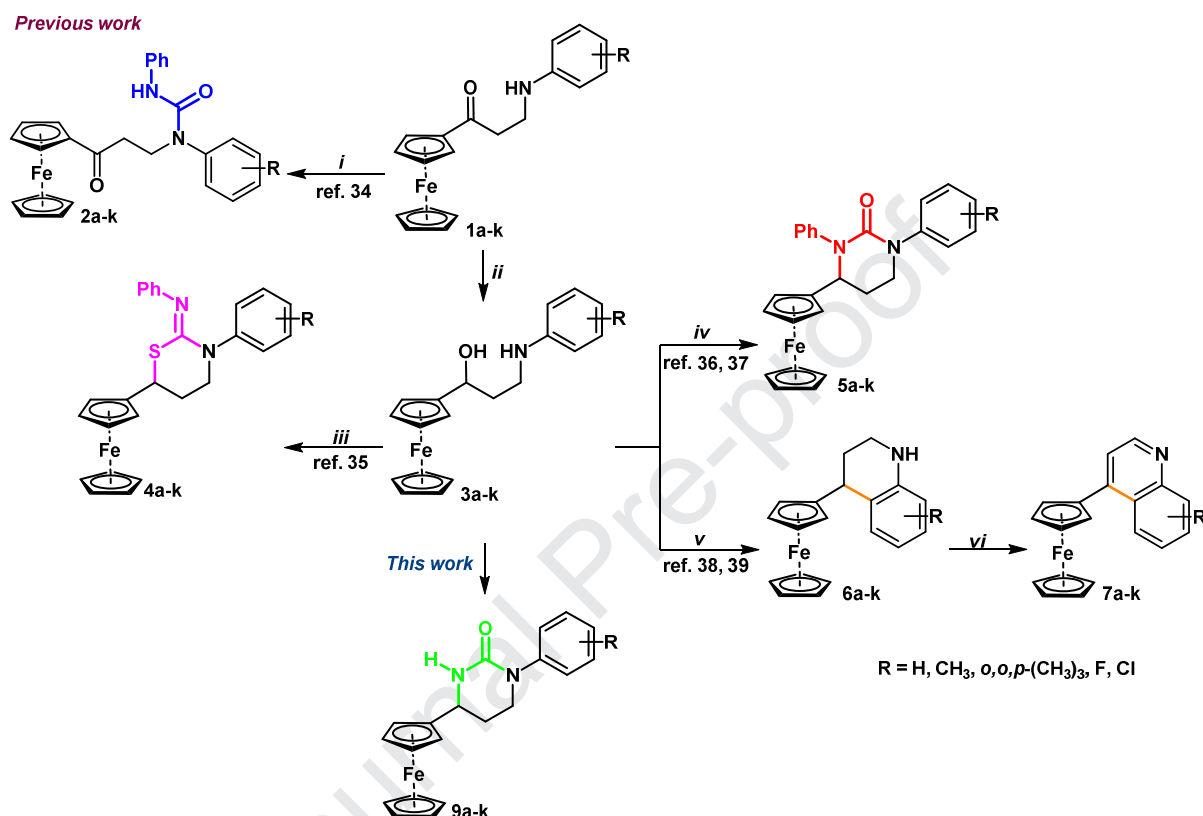
## 1. Introduction

In recent years we have seen an increased interest of both chemists and biologists for urea derivatives, which have been synthesized extensively since. This specific class of compounds is characterized by a wide range of biological activities, therefore, urea derivatives represent promising candidates as anticonvulsant [1], antibacterial [2], antitumor [3], anti-HIV [4], antagonistic [5], anti-proliferative [6], anticancer (renal cancer, colon cancer, lungs cancer, prostate cancer, and breast cancer) [7], and antifungal [8] agents. Besides, urea derivatives have been used as organocatalysts in organic synthesis [9] and have been applied in material science [10], which has consequently resulted in a heightened interest for their synthesis.

Since its discovery in 1951 [11], ferrocene (Fc) and its derivatives have found applications in many areas, among which the most important are in material science, asymmetric catalysis, bioorganometallic chemistry, and organic synthesis [12]. The incorporation of ferrocene nucleus into biologically relevant molecules can significantly enhance molecular properties such as solubility, hydrophobicity and lipophilicity of '*parent compounds*' [13]. Consequently, many Fc-containing compounds exhibit antimalarial [14], antifungal [15], anti-HIV, and DNA cleaving activity [16], as well as antitumor activity [17–20]. Thus, the ferrocene moiety was recognized as an attractive pharmacophore in drug design [21] and a multitude of reports dealing with derivatives of this metallocene have been appeared in the literature.

In continuation of our long-standing interest toward the synthesis of Fc-containing compounds [22–24], particularly those that contain heterocyclic core and represent potentially bioactive agents [25–31], we developed protocols for obtaining 3-(arylamino)-1-ferrocenylpropan-1-ones [32, 33]. 3-(Arylamino)-1-ferrocenylpropan-1-ones – Mannich bases have demonstrated the great results in the synthesis of Fc derivatives, giving rise to five different series of novel acyclic and heterocyclic ferrocene compounds (see Scheme 1). Thus, using Mannich bases as starting material we successfully designed strategies and optimized reaction conditions for the synthesis of 1-aryl-1-(3-ferrocenyl-3-oxopropyl)-3-phenylureas (**2a-k**) [34], 3-aryl-6-ferrocenyl-*N*-phenyl-1,3-thiazinan-2-imines (**4a-k**) [35], 1-aryl-4-ferrocenyl-3-phenyltetrahydropyrimidin-2(1*H*)-ones (**5a-k**) [36, 37], 4-ferrocenyl-1,2,3,4-tetrahydroquinolines (**6a-k**) and 4-ferrocenylquinolines (**7a-k**) (see Scheme 1) [38, 39]. Notably, as it can be seen on Scheme 1, particular attention of our research group has been paid to the reaction between reduced Mannich bases **3a-k** and organic iso(thio)cyanate [35–

37]. Bearing in mind all above mentioned, previously obtained experience, we have been encouraged to expand our studies and test the application of the corresponding 1,3-amino alcohol **3a-k** in reaction with cyanate salt (see Scheme 1). Therefore, in this paper the focus was on designing a synthetic strategy for the preparation of Fc-containing tetrahydropyrimidin-2(1*H*)-ones by reaction between reduced Mannich base **3a-k** and cyanate salt.



**Scheme 1.** Synthesis of Fc-containing compounds starting from Mannich bases. Reagents and conditions: *i*) PhNCO, ultrasound irradiation for 1h; *ii*) NaBH<sub>4</sub>, MeOH, stirring for 2h; *iii*) PhNCS, ultrasound irradiation (1-7 h), then AcOH, ultrasound irradiation, 1 h; *iv*) PhNCO, ultrasound irradiation, 1 h, and then AcOH, ultrasound irradiation, 1 h; *v*) AcOH, ultrasound irradiation, 2 h; *vi*) DDQ, toluene, reflux for 2 h.

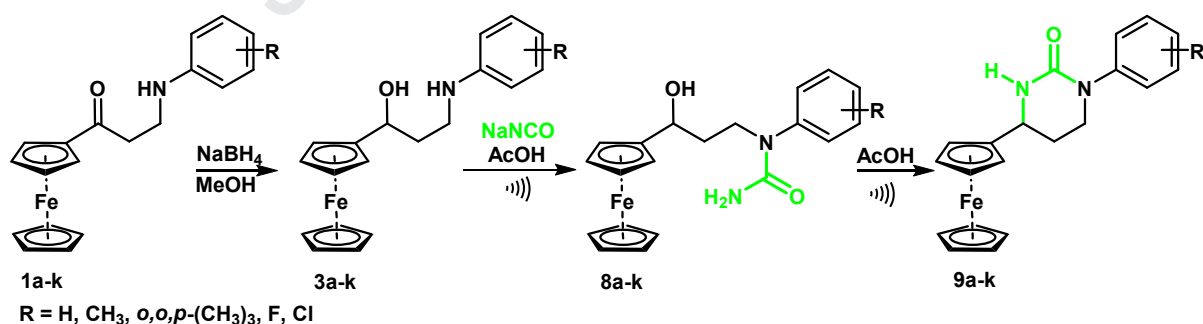
In view of this, growing interest in urea derivatives has prompted the development of protocols for their synthesis and most of them are based on the reaction of carbon dioxide (CO<sub>2</sub>), carbon monoxide (CO) and phosgene (COCl<sub>2</sub>) with amines [40]. However, a numerous of other synthetic pathways have been developed to obtain this class of compounds. Among them, reactions of amines with organic isocyanates characterized by mild conditions and high product yields have been identified as the most effective and widely applied strategy for the synthesis of urea derivatives [41, 42]. In accordance with that, in the present paper, we report the preparation of eleven novel 1-aryl-4-ferrocenyltetrahydropyrimidin-2(1*H*)-ones achieved *via* a one-pot reaction between

3-arylamino-1-ferrocenylpropan-1-ols and sodium cyanate (NaOCN) in the presence of glacial acetic acid. All products were purified by column chromatography and their structures were confirmed by spectroscopic data ( $^1\text{H}$  NMR,  $^{13}\text{C}$  NMR, 2D NMR and IR). Moreover, a detailed single-crystal X-ray diffraction analysis has been successfully performed on three representative examples, as well as elemental analysis. In addition, electrochemical behavior of all synthesized compounds has been investigated using cyclic voltammetry technique.

## 2. Results and Discussion

### 2.1. Synthesis of 1-aryl-4-ferrocenyltetrahydropyrimidin-2(1H)-ones (**9a-k**)

Within the first phase of this study, we made sure to establish an appropriate method for the synthesis of 1-aryl-4-ferrocenyltetrahydropyrimidin-2(1H)-ones. Our research team has been already designed a strategy and optimized reaction conditions for the synthesis of Fc-derivatives of six-membered cyclic ureas in high-to-excellent yields [36, 37]. This synthesis involved the reaction between the corresponding 1,3-amino alcohols **3a-k** and phenyl isocyanate and the subsequent intramolecular cyclization of generated 1,3-hydroxyureas in the presence of glacial acetic acid. According to literature [43, 44], the reaction between the amino group and the cyanate salt undergoes in acidic medium building the corresponding urea derivatives. In this manner, we designed the protocol for the synthesis of cyclic ureas **9a-k** through the usage of sodium cyanate. Thus, we set “*order of events*” – 3-(arylamino)-1-ferrocenylpropan-1-ols  $\rightarrow$  3-(arylamino)-1-ferrocenylpropan-1-ols  $\rightarrow$  1-aryl-1-(3-ferrocenyl-3-hydroxypropyl)ureas  $\rightarrow$  1-aryl-4-ferrocenyltetrahydropyrimidin-2(1H)-ones (see Scheme 2).

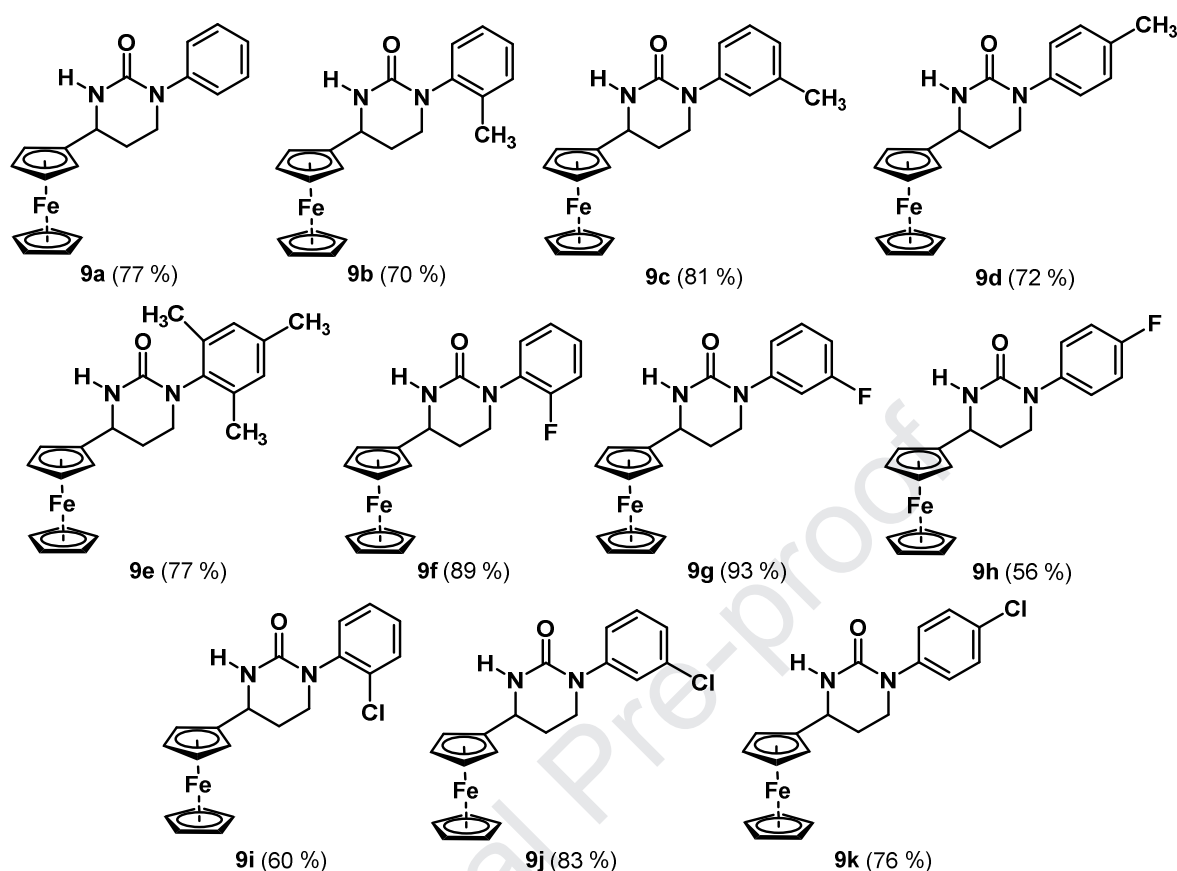


**Scheme 2.** A synthetic strategy to 1-aryl-4-ferrocenyltetrahydropyrimidin-2(1H)-ones (**9a-k**)

A synthetic strategy included the preparation of 1,3-amino alcohols **3a-k** by reduction of 3-(arylamino)-1-ferrocenylpropan-1-ones (**1a-k**), and then an intramolecular cyclization of *in situ* generated 1,3-hydroxyureas **8a-k** (see Scheme 2). The reduction of Mannich bases **1a-k** was performed very smoothly and the corresponding 1,3-amino alcohols **3a-k** were obtained in high yields [36]. In order to establish optimal conditions, we set up the reaction between **3a** (1 mmol) and sodium cyanate (1.5 mmol). The reaction mixture was placed in an ultrasound bath for 2 hours at ambient temperature. Sequentially, glacial acetic acid (1 ml) was added in the well homogenized mixture and the irradiation was continued for 2 hours. After the usual workup and column chromatography (SiO<sub>2</sub>/n-hexane–EtOAc, 1:1, v/v), these reaction conditions successfully yielded **9a** and the promised heterocyclic scaffold is isolated in 77% yield. This result suggested that the reaction proceeds in a *one-pot* manner *via* 1,3-hydroxyurea **8a**. Further, these reaction conditions have not required additional screening and have been accepted as optimal ones. The scope of the reaction has been investigated employing ten additional 3-(arylamino)-1-ferrocenylpropan-1-ols **3b-k**. The desired products **9a-k** have been obtained in moderate to excellent yields (up to 93%) after the purification by means of column chromatography (see Scheme 3). Structural characterization has been confirmed by spectroscopic methods (NMR, IR), as well as elemental analysis, and revealed a purity of >95% for all prepared compounds.

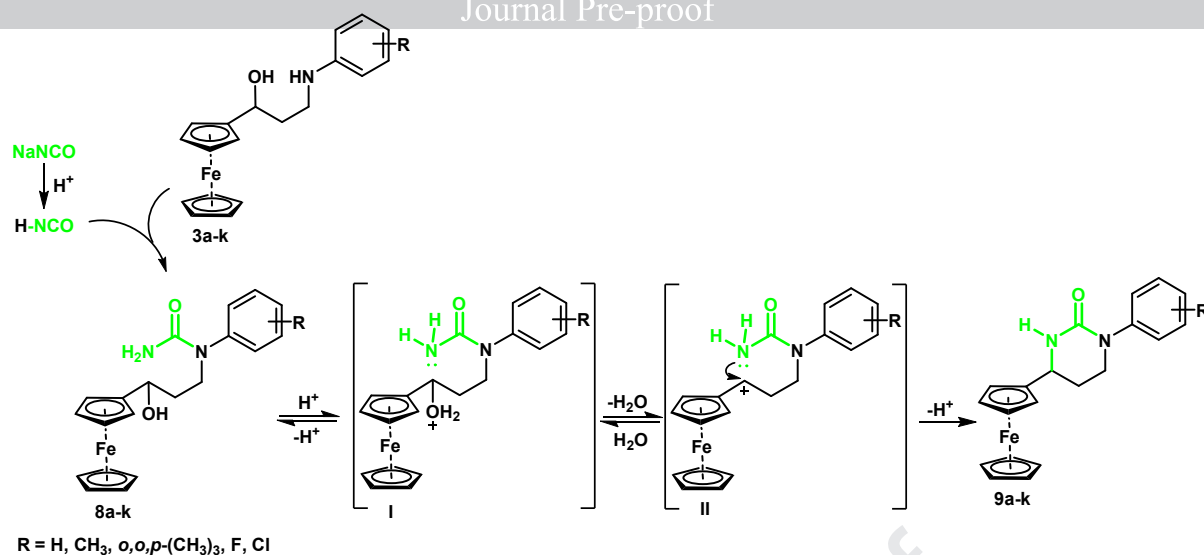
We have observed that the electronic properties of the substituents of the phenyl group have a significant influence on reaction outcomes (see Scheme 3). Regarding that, the products obtained from substrates with an electron-withdrawing group on the phenyl ring, as well as *ortho*-substituted phenyl group were isolated in lower yield (see Scheme 3). Consequently, the steric hindrance also has an influence on the reaction outcome since 1,3-amino alcohols with a bulky substituent in the *ortho*-position of the phenyl group leads to moderate yield (see Scheme 3, products **9b** and **9i**). In addition, 1,3-amino alcohol **3b** with a methyl group in the *ortho*-position of the phenyl group gives **9b** which exists in two pairs of enantiomers due to the presence of atropisomerism. This observation is consistent with our previous reports [36, 37]. The isomerism is caused by the resonance of the carbonyl diamide functional group which restricts rotation around the single bond between the nitrogen of the heterocyclic ring and the carbon of the aryl group [36, 37]. Based on the <sup>1</sup>H NMR spectrum of **9b**, the ratio of diastereoisomers is approximately 1:1. A comparison of results obtained within this study with previous results suggests that the substituent on the second nitrogen atom of the cyclic urea fragment has a significant influence on the rigidity of the ring [36,

37]. Therefore, a more flexible tetrahydropyrimidinone ring of **9a-k** can explain the absence of the expected atropisomerism in product **9i**.



**Scheme 3.** An overview of newly Fc-containing tetrahydropyrimidin-2(1*H*)-ones **9a-k**

Reaction mechanism has been discussed to get a more comprehensive insight into the *in situ* generation of 1,3-hydroxyureas, as well as the role of  $\alpha$ -ferrocenyl carbocation in intramolecular cyclization. Initially, cyanic acid is generated from sodium cyanate in acidic medium (see Scheme 4). In the next step, the amino group of 1,3-amino alcohols **3a-k** is added to cyanic acid building the corresponding 1,3-hydroxyureas **8a-k** [43–45]. The reaction pathway continues with the protonation of 1,3-hydroxyureas giving oxonium ions **I**. Further,  $\alpha$ -ferrocenyl carbocations **II** were formed by dehydration of oxonium ions **I**. Noteworthy,  $\alpha$ -ferrocenyl carbocations **II** are known as very stable due to the participation of ferrocenyl moiety in the delocalization of positive charge [12, 46]. In the last step, a nucleophilic attack of the carbamide nitrogen on the positive center of cations **II** affords products **9a-k**.



**Scheme 4.** Plausible schematic mechanism for the synthesis of titled compounds **9a-k**

## 2.2. Spectral characterization

The newly synthesized 1-aryl-4-ferrocenyltetrahydropyrimidin-2(1*H*)-ones (**9a-k**) were found to be stable at the room temperature for a prolonged time and could safely be handled in air, but like other ferrocene derivatives, they should be stored in closed containers. To confirm their structure, a detailed characterization has been done by standard spectroscopic techniques (IR, <sup>1</sup>H and <sup>13</sup>C NMR), as well as elemental analysis. All collected spectral data were fully consistent with the proposed structures (for more data see Experimental part and *ESI*).

The IR spectra of Fc-derivatives **9a-k** contain the medium intensity absorptions of NH stretching vibrations at 3419–3438 cm<sup>-1</sup>, indicating that all NH groups are involved in the H-bonding interactions. The characteristic bands at 1646–1670, 1495–1610 and 1448–1590 cm<sup>-1</sup> have been most likely originated from carbonyl diamide group. Moreover, the IR spectra of example **9a** have been presented on the Figure 1 (for more data see Experimental part and for copies of IR spectrums for all prepared compounds see *ESI*).

Three sets of signals have been observed in the <sup>1</sup>H NMR spectra. The first belongs to protons of the tetrahydropyrimidinone moieties, the second to the aromatic protons and the third to protons of the ferrocene units (see Figure 2). The signals at ~ 3.28–3.84 and 1.76–2.34 ppm originate from the protons of the methylene groups (H-6a, H-6b, H-5a, and H-5b, respectively), while the characteristic doublets of doublets at ~ 4.40 ppm belong to the protons of the methine groups (H-4) in the heterocyclic rings. Also, the broad singlets at ~ 5.30 ppm assigned to the corresponding protons of NH fragments in the ring (H-3). The overlapped multiplets at 4.11–4.33 ppm originate from the protons of the substituted

cyclopentadiene rings (H-2'', H-3'', H-4'' and H-5''), and the singlets at  $\sim 4.22$  ppm belong to the protons of unsubstituted ferrocene cyclopentadiene rings (H-1''') in the  $^1\text{H}$  NMR spectra. The signals of aromatic protons (H-2', H-3', H-4', H-5' and H-6') are located at the expected chemical shifts ( $> 6.80$  ppm) in the spectra (see Experimental part and *ESI*). Further, signals assigned to the corresponding carbons of the synthesized compounds **9a-k** appear in the expected regions of the  $^{13}\text{C}$  NMR spectra. Moreover, the presence of signal at around 155 ppm (C-2) in the  $^{13}\text{C}$  NMR spectra of **9a-k** unambiguously confirmed the proposed product structure and intramolecular *N*-alkylation, since this signal belongs to carbon of the carbamide functional group (for more data see Experimental part and *ESI*).

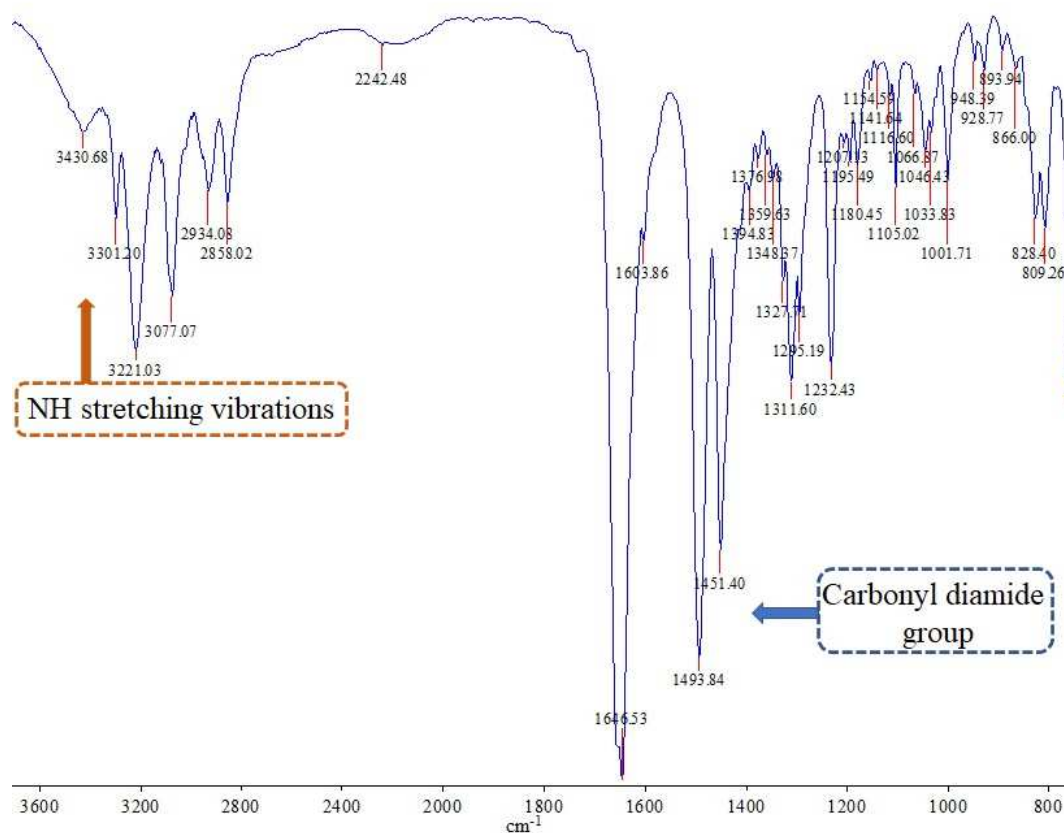


**Figure 1.** The IR spectra ( $800\text{-}3600\text{cm}^{-1}$ ) for compound **9a**

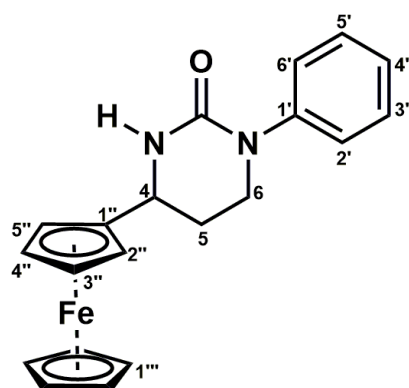


**Figure 2.** Labeled carbons atoms for NMR characterization

The compounds **9d**, **9h** and **9j** have been characterized by single-crystal X-ray diffraction analysis. The molecular structure and the atom labelling scheme are presented in Figure 3, while the selected bond lengths and angles are listed in Table 1. The X-ray analysis reveals similar composition of the three compounds where the central six-membered cyclic urea links the ferrocene moiety in position C11 and *p*-CH<sub>3</sub>, *p*-F and *m*-Cl substituted phenyl ring in position N1 (Figure 3). The ferrocene units display only slight geometrical distortion. Each pair of cyclopentadienyl (Cp) rings takes close to parallel orientation, with the maximum dihedral angle between the mean planes of 2.0(1)° found in compound **9j**. The Cg1–Fe–Cg2 angle of the same compound (177.9°) also shows the maximum deviation from the ideal geometry (Cg1 and Cg2 are centroids of the substituted and unsubstituted Cp rings, respectively). The distances between the Fe atom and the Cg1 and Cg2 centroids are: 1.654/1.645, 1.648/1.641, 1.649/1.644 Å in **9d**, **9h** and **9j**, respectively. The more pronounced difference between the Fc units is observed for the C1–Cg1–Cg2–C6 torsion angle which indicates the conformational changes from almost eclipsed in **9d** (–7.0°) to staggered in **9h** and **9j** (–21.9 and 27.0°, respectively).

In all cases, the cyclic urea is significantly rotated with respect to the Cp1 plane. This is illustrated by the large dihedral angle between the best plane through the five approximately coplanar atoms of the heterocycle, N1–N2–C11–C12–C13 and the corresponding Cp1 ring which is 66.7(1), 67.9(1) and 70.7(1)° in **9d**, **9h** and **9j**, respectively. The displacement of the remaining C14 atom from the N1–N2–C11–C12–C13 plane is significant and equals to 0.621(4), 0.623(4), 0.640(3) Å in **9d**, **9h** and **9j**, respectively. The dihedral angle between the planes of cyclic urea and the phenyl ring in position N1 is 27.7(1), 28.3(1) and 21.6(1)° in **9d**, **9h** and **9j**, respectively. All these parameters indicate a great structural similarity of the three compounds, which is also confirmed by an overlay of their molecular structures presented in Figure 4a.

It is interesting to compare the conformational features of the present compounds with those of the four previously reported ferrocene-containing six-membered cyclic ureas where the H atom in position N2 is replaced with an additional phenyl substituent [36, 37]. Apart from the increased dihedral angle between the N1–N2–C11–C12–C13 and Cp1 planes, which in the N2-substituted structures approaches to 90°, these structures are characterized by a completely different orientation of the urea ring. The overlay of molecular structures of the compound **9d** and one of the previously reported N2-substituted derivatives presented in Figure 4b emphasizes the conformational difference in two groups of compounds. Thus, in

the N2-substituted structures [36, 37], the ureido N2 lies approximately in the level of Cp1 plane (average displacement of 0.07 Å) dissimilar to **9d**, **9h** and **9j**, where the same atom deviates up to 1.42 Å from this plane. Opposite was found for C14 (average displacement of 1.37 in N2-substituted and 0.30 Å in current structures). Also, in N2-substituted structures the carbonyl O atom points away from the Fc moiety, with the average displacement from the Cp1 plane of 1.14, while in **9d**, **9h** and **9j**, the same atom orients orthogonally to Cp1 with the extreme deviation of 3.06 Å in average (see Figure 4b).

Additional overlay of the derivatives, based on the atoms of cyclic urea, is given in Figure S1 (see *ESI*). It actually reveals that the altered orientation of the cyclic urea with respect to the Cp1 ring results from the fact that Fc moiety occupies the axial position of the heterocycle in **9d**, **9h** and **9j**, while the equatorial position in N2-substituted derivatives. The same overlay also indicates a considerable conformational similarity of the heterocycle in all crystal structures. Namely, each heterocycle is characterized by an approximately planar N1–N2–C11–C12–C13 fragment resulting from the trigonal character of the two N atoms and the delocalization of electron density in the ureido fragment. The atom C14 shows significant displacement from the N1–N2–C11–C12–C13 plane which ranges from 0.621(4) in **9d** to 0.709(5) [37]. Also, the valence angles in the cyclic urea show wide range of values from 107 at  $sp^3$  C up to 127 at  $sp^2$  N atoms.

The geometrical parameters listed in Table 1 show only minor mutual differences between the **9d**, **9h** and **9j**. The maximum variations are observed in N1–C12 bond (0.008 Å) and in the C12–N1–C15 angle involving the phenyl substituent (1.3°). In comparison to the values in Table 1, the N2-substituted derivatives display small but systematic differences, especially in the half of the ring bearing the additional phenyl substituent. Thus, compared to title compounds, the C12–N2 and C11–C14 bonds in N2-substituted structures are longer for 0.04 and 0.02 Å in average, respectively. Also, the C12–N2–C11 angle is larger for 4° in average, mainly on expense of the C12–N1–C13 angle which narrows for the same average value.

The crystal structures of **9d**, **9h** and **9j** display similar packing features. The hydrogen bond formed between the N2-donor and the ureido oxygen acceptor represents the dominate interaction in three crystal structures (see Table 2). By this interaction, the inversion related molecules arrange into pairs generating the cyclic  $R^2_2(8)$  motifs (see Figure 5). The ferrocenyl units of the N2–H...O1 bonded molecules, self-organize into additional pairs forming the rigid ferrocene-ferrocene dimers. Through the combination of N2–H...O1 hydrogen bonding and Fc...Fc interaction the molecules arrange into double chain which

extends along the *c* crystallographic axis of the corresponding unit cells (Figure 5, see *ESI*: Figure S2 and Figure S3). One should notice that the Fc...Fc dimer represents the only interaction which exists in current as well as in N2-substituted derivatives. This confirms the stability and persistence of the Fc...Fc building blocks [47], regardless the different conformation of ferrocene derivatives or the presence of strong hydrogen bonds.

In contrast to **9d**, **9h** and **9j**, the lack of an adequate hydrogen bonding donor in N2-substituted derivatives [36, 37] prevents the formation of strong hydrogen bond, hence the ureido O1 serves as an acceptor only in weak C–H...O interactions. The Hirshfeld fingerprint plots [48] presented in Figure. S4 (see *ESI*) emphasize the difference in intermolecular interactions for the two groups of derivatives. The most prominent feature of the mutually similar plots of **9d**, **9h** and **9j** is a pair of sharp spikes belonging to N2–H...O1 hydrogen bond. Contrary, in the plots of N2-substituted derivatives the spikes of C–H...O are weakly expressed. The presence of lateral ‘wings’ in each plot (see *ESI* Figure S4) indicates the importance of weak C–H... $\pi$  interactions for both types of derivatives. Nevertheless, the different molecular conformations employ dissimilar C–H donors and  $\pi$ -acceptors for this type of interactions. The **9d**, **9h** and **9j**, form equivalent set of C–H... $\pi$  interactions (see Table 2). The most important interaction of this type is C4–H... $\pi$  which employs C–H donor from the substituted Cp ring and the phenyl ring as  $\pi$ -acceptor. This interaction leads to the further paring of the centrosymmetric molecules and interconnection of the above described double chains (see *ESI* Figure S5).

**Table 1.** Selected bond lengths (Å) and angles (°) in crystal structure of **9d**, **9h** and **9j**.

	<b>9d</b>	<b>9h</b>	<b>9j</b>
O1–C12	1.231(3)	1.235(3)	1.228(2)
N1–C12	1.383(3)	1.380(3)	1.391(2)
N1–C15	1.428(3)	1.425(3)	1.422(2)
N1–C13	1.473(3)	1.472(3)	1.474(2)
N2–C12	1.343(3)	1.347(3)	1.348(2)
N2–C11	1.462(3)	1.459(3)	1.464(2)
C1–C11	1.503(3)	1.503(3)	1.504(2)
C11–C14	1.504(3)	1.510(4)	1.503(3)
C13–C14	1.516(3)	1.514(4)	1.517(3)
C12–N1–C15	120.59(18)	121.1(2)	121.90(14)
C12–N1–C13	120.32(18)	120.2(2)	120.28(14)
C15–N1–C13	118.35(17)	117.6(2)	117.33(14)
C12–N2–C11	126.9(2)	126.8(2)	126.69(15)
C5–C1–C11	128.8(2)	129.0(2)	128.56(17)
C2–C1–C11	124.2(2)	123.5(2)	124.17(17)
N2–C11–C1	107.72(18)	108.0(2)	108.47(14)
N2–C11–C14	107.25(18)	107.0(2)	107.01(15)
C1–C11–C14	115.71(19)	115.6(2)	114.96(16)
O1–C12–N2	120.8(2)	120.5(2)	120.75(16)
O1–C12–N1	121.9(2)	122.1(2)	122.06(16)
N2–C12–N1	117.22(19)	117.4(2)	117.17(15)
N1–C13–C14	110.80(18)	110.8(2)	111.12(14)
C11–C14–C13	110.19(19)	110.2(2)	109.72(16)

**Table 2.** Geometry of intermolecular interactions in crystal structure of **9d**, **9h** and **9j**.

	D–H (Å)	H...A (Å)	D–H...A (°)	Symmetry code:	
<b>9d</b>	N2–H2...O1	0.76(3)	2.14(3)	176(3)	$-x+1, -y+2, -z+1$
	C4–H4...Cg3	0.93	2.83	145	$x, y, z+1$
	C11–H11...Cg3	0.98	3.14	139	$-x+2, -y+2, -z+1$
	C17–H17...Cg2	0.93	3.18	159	$x, y, z-1$
<b>9h</b>	N2–H2...O1	0.78(3)	2.17(3)	172(3)	$-x+1, -y+2, -z$
	C4–H4...Cg3	0.93	2.90	144	$-x+1, -y+1, -z$
	C11–H11...Cg3	0.98	3.15	136	$-x, -y+2, -z$
	C13–H13a...Cg1	0.97	3.15	128	$x+1, y, z$
	C17–H17...Cg2	0.93	2.82	179	$x, y, z+1$
<b>9j</b>	N2–H2...O1	0.83(3)	2.10(3)	176(2)	$-x+2, -y+1, -z+1$
	C4–H4...Cg3	0.93	2.80	142	$-x+2, -y, -z+1$
	C11–H11...Cg3	0.98	3.13	130	$-x+1, -y+1, -z+1$
	C13–H13a...Cg1	0.97	3.07	130	$x+1, y, z$

Cg1 and Cg2 are centroids of the substituted and unsubstituted Cp rings, respectively; Cg3 is centroid of phenyl ring.

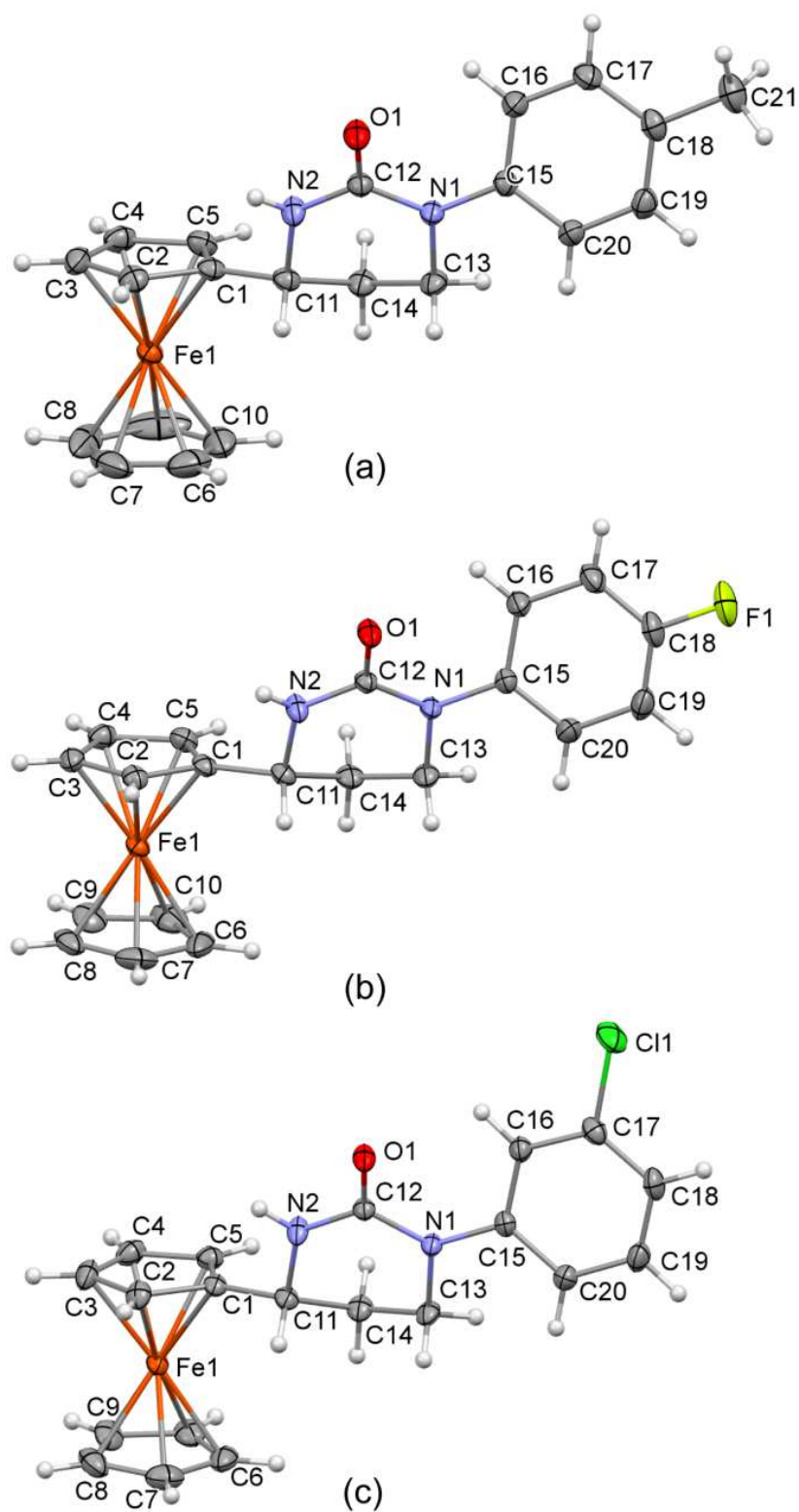


**Figure 3.** The molecular structure with the atom-labelling scheme: (a) **9d**, (b) **9h** and (c) **9j**. Displacement ellipsoids are drawn at the 30% probability level.

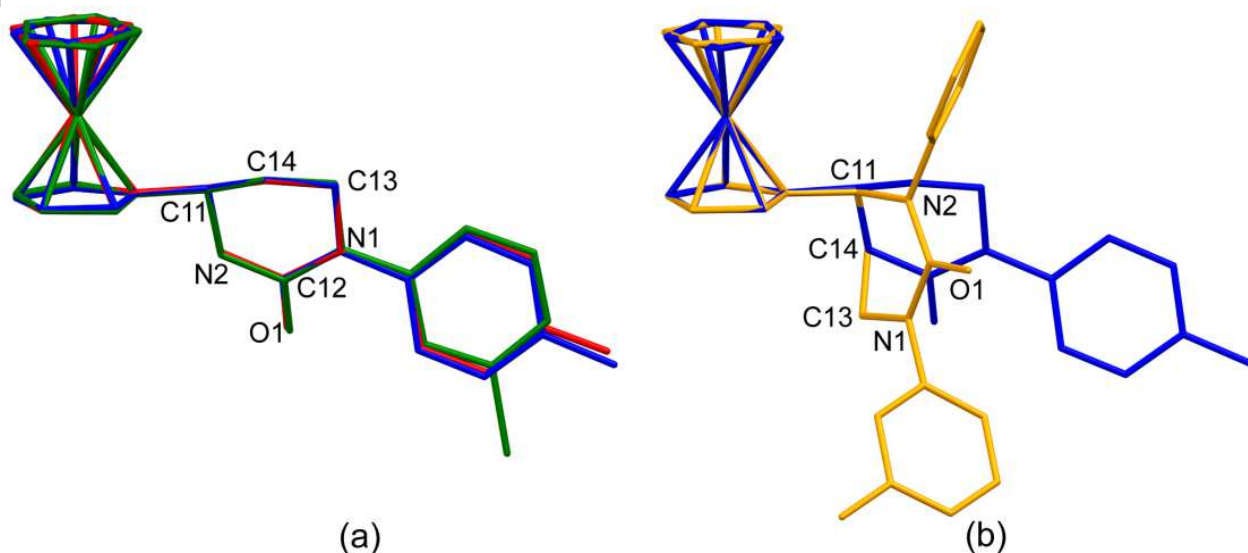


**Figure 4.** (a) Overlay of **9d**, **9h** and **9j** (blue, green and red, respectively) based on the atoms of Cp1 ring. Overlay of **9d** (blue) and the N2-substituted derivative [36] (yellow); atom-labelling scheme in (b) corresponds only to the yellow colored molecule, atom-labelling of **9d** is as in (a) where this molecule is presented in the same orientation. H atoms are excluded for clarity.

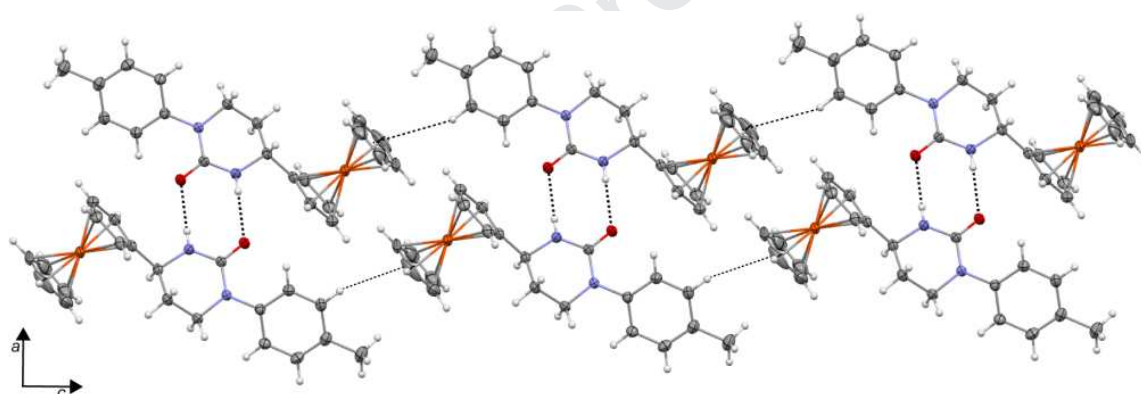


**Figure 5.** Double chain of **9d** molecules formed by N2–H...O1 hydrogen bond, Fc...Fc pairing and C17–H... $\pi$  interaction. Equivalent chains for **9h** and **9j** are presented in Figure S2 and Figure S3 (see *ESI*).

It is well known that the  $\text{Fe}^{2+}/\text{Fe}^{3+}$  redox chemistry contributes to the bioactivity of ferrocene derivatives [26-31, 49 and 50]. Led by this fact, we opted to evaluate the electrochemical properties of all newly prepared compounds **9a-k**. This has been done by means of cyclic voltammetry (CV) in dichloromethane containing 0.1 mol/L tetrabutylammonium perchlorate as a supporting electrolyte. The working electrode was a polished platinum disk (2 mm diameter; Metrohm). The counter electrode was a platinum wire, whereas an Ag/AgCl electrode was used as the reference. The peak potentials ( $E_p$ ) of the anodic and cathodic potentials ( $E_{pa}$  and  $E_{pc}$ , respectively, at  $0.1 \text{ V s}^{-1}$ ), their half-wave potentials ( $E_{1/2} = (E_{pa} + E_{pc})/2$ ), and the differences between anodic and cathodic peak potentials ( $\Delta E = E_{pa} - E_{pc}$ ) of Fc-derivatives **9a-k**, have been measured and evaluated as important electrochemical data [52]. All measurements have been carried out using ferrocene as internal standard. Besides, an additional proof of purity for all synthesized compounds has been provided by CV measurements.

#### 2.4.1. Redox behavior of prepared 1-aryl-4-ferrocenyltetrahydropyrimidin-2(1H)-ones (**9a-k**)

The redox behavior of the products **9a-k** has been determined using cyclic voltammetry (CV) under the same conditions mentioned above, and the results of this study have been listed in Table 3. Based on collected data, we have determined that all novel Fc-containing derivatives **9a-k** exhibited one well-defined oxidation wave on the forward-potential sweep (0.662 – 0.729 V) and one reduction wave during the back-potential sweep (0.461 – 0.543 V) assigned to the ferrocene nucleus. It appears that the oxidation potentials of **9a-k** have been more positive than the ones of the unsubstituted ferrocenes (for representative example see Figure 6), which shows significant electronic contact between the ferrocene unit and the rest of the molecule. Due to the reversibility of this electron transfer, even at low scan speed, the produced radical anion is stable within the time scale of cyclic voltammetry (see Figure 7) [51]. Both anodic and cathodic peak currents are proportional to the square root of the scan rate (see Figure 8), and their ratio is independent of the scan rate, indicating a diffusion-controlled process. Moreover, the average of anodic and cathodic current was not unity and the difference between the oxidation and reduction maxima ( $\Delta E = E_{pa} - E_{pc}$ ) was around 0.168 V. Compared with the theoretical value  $\Delta E = 0.150 \text{ V}$ , we can determine that the redox process is quasi-reversible nature [51].

**Table 3.** The electrochemical data for compounds **9a-k**

Entry	Compound	$E_{pa}^a$ (V)	$E_{pc}^a$ (V)	$E_{1/2}^b$ (V)	$\Delta E^c$ (V)
1	<b>9a</b>	0.729	0.461	0.595	0.268
2	<b>9b</b>	0.659	0.510	0.585	0.149
3	<b>9c</b>	0.665	0.522	0.594	0.143
4	<b>9d</b>	0.668	0.528	0.598	0.140
5	<b>9e</b>	0.684	0.497	0.591	0.187
6	<b>9f</b>	0.668	0.513	0.591	0.155
7	<b>9g</b>	0.720	0.491	0.606	0.229
8	<b>9h</b>	0.662	0.543	0.603	0.119
9	<b>9i</b>	0.687	0.504	0.596	0.183
10	<b>9j</b>	0.684	0.528	0.606	0.156
11	<b>9k</b>	0.668	0.543	0.606	0.125

<sup>a</sup>  $E_{pa}$  and  $E_{pc}$  anodic and cathodic peak potentials, respectively, at  $0.1 \text{ V s}^{-1}$ .

<sup>b</sup>  $E_{1/2} = (E_{pa} + E_{pc})/2$ .

<sup>c</sup>  $\Delta E = E_{pa} - E_{pc}$ .

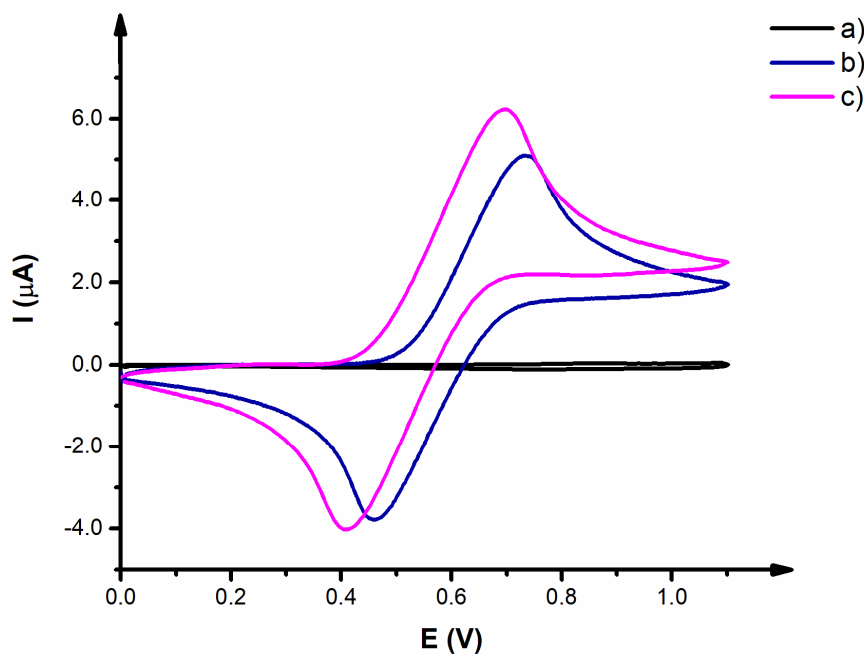


**Figure 6.** Cyclic voltammograms at the platinum disk ( $d = 2 \text{ mm}$ ) by a  $0.1 \text{ V s}^{-1}$  scan rate in  $0.1 \text{ M}$  dichloromethane solution of  $\text{Bu}_4\text{NClO}_4$ : (a) electrolyte, (b)  $1 \text{ mM}$  solution of 4-ferrocenyl-1-phenyltetrahydropyrimidin-2(1H)-one (**9a**) (c) ferrocene.

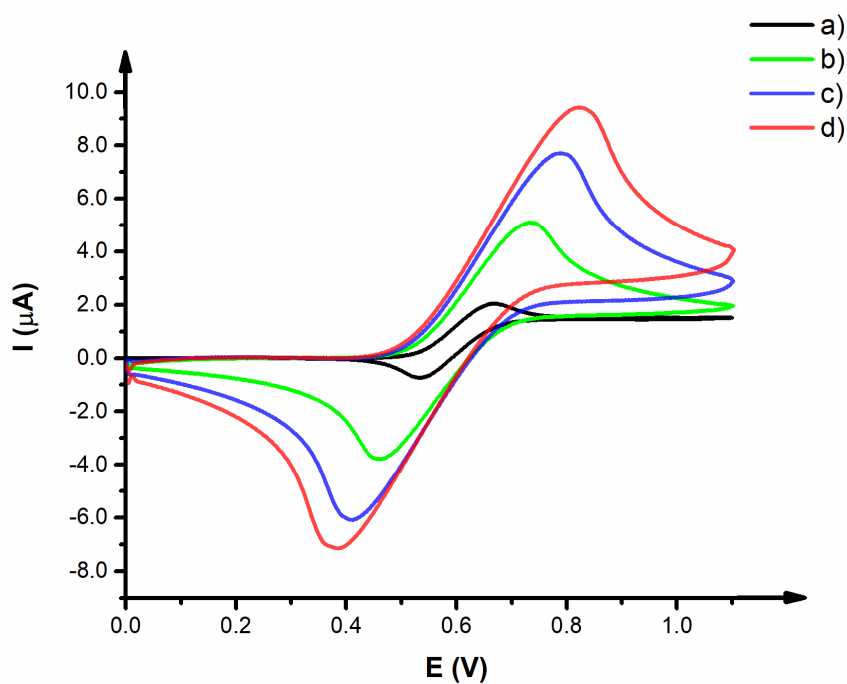


**Figure 7.** Cyclic voltammograms of 1 mM solution of 4-ferrocenyl-1-phenyltetrahydropyrimidin-2(1*H*)-one (**9a**) at the platinum disk ( $d = 2$  mm) in 0.1 M dichloromethane solution of  $\text{Bu}_4\text{NClO}_4$  on a different scan rates: a)  $0.01 \text{ V s}^{-1}$  b)  $0.1 \text{ V s}^{-1}$  c)  $0.3 \text{ V s}^{-1}$  d)  $0.5 \text{ V s}^{-1}$

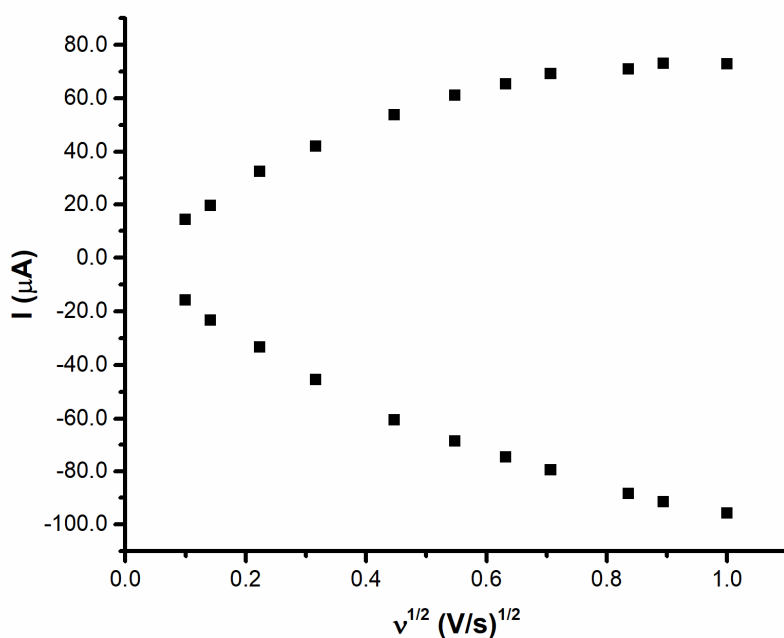


**Figure 8.** Anodic and cathodic peak currents of product **9a** obtained at different scan rates at the platinum disk ( $d = 2$  mm) in 0.1 M dichloromethane solution of  $\text{Bu}_4\text{NClO}_4$ .

### 3. Conclusion

In summary, we have described a new, easily performable *one-pot* procedure for the synthesis of Fc-containing tetrahydropyrimidin-2(1*H*)-ones in good to excellent yields (up to 93%) starting from 3-(arylamino)-1-ferrocenylpropan-1-ols and sodium cyanate (NaNCO) in acidic medium. The reported protocol is practical and convenient and proceeds under relatively mild conditions – an ultrasound irradiation has been used as reaction promoter and acetic acid has been applied as catalyst. The structures of novel compounds are determined using standard spectroscopic methods (IR and NMR). The proposed structures of three representative products **9d**, **9h** and **9j** are confirmed by single-crystal X-ray diffraction analysis, as well as by elemental analysis. Further, the cyclic voltammetry studies were done in order to evaluate electrochemical behavior of the prepared ferrocenes. This investigation has revealed that all products **9a-k** exhibit only one well-defined redox couple (attributed to the ferrocene nucleus). In addition, the presented synthetic approach, besides practical application, gives rise to new potentially biologically relevant Fc-containing six-membered cyclic ureas.

## 4. Experimental

### 4.1. General information

All chemicals were commercially available and used as received, except the solvents, which were purified by distillation. Ultrasonic cleaner Elmasonic S 10 (Elma, Germany), 30W was used for the ultrasonically supported synthesis. Chromatographic separations were carried out using silica gel 60 (Merck, 230–400 mesh ASTM), whereas silica gel 60 on Al plates, (Merck, layer thickness 0.2 mm) was used for TLC. The  $^1\text{H}$  and  $^{13}\text{C}$  NMR spectra of the samples in  $\text{CDCl}_3$  were recorded on a Bruker Avance III 400 MHz ( $^1\text{H}$  at 400 MHz,  $^{13}\text{C}$  at 101 MHz) and Varian Gemini ( $^1\text{H}$  at 200 MHz,  $^{13}\text{C}$  at 50 MHz) NMR spectrometers. Chemical shifts are expressed in  $\delta$  (ppm), relative to residual solvent protons as the internal standard ( $\text{CDCl}_3$ : 7.26 ppm for  $^1\text{H}$  and 77 ppm for  $^{13}\text{C}$ ). The coupling constants ( $J$ ) are reported in Hz. Multiplicities of proton resonance are designated as singlet (s), broad singlet (br s), doublet (d), broad double (br d), doublet of doublets (dd), triplet (t), doublet of triplets (dt), doublet of doublets of doublets (ddd), quartet (q) and multiplets (m). 2D NMR experiments ( $^1\text{H}$ - $^1\text{H}$  COSY, NOESY, HSQC and HMBC) are performed on the same instrument with a standard pulse sequence. IR measurements were carried out with a Perkin–Elmer FTIR 31725-X spectrophotometer. Microanalyses of carbon, hydrogen and nitrogen were carried out with a Carlo Erba 1106 model microanalyzer; these results agreed favorably with the calculated values. Melting points were determined on a Mel-Temp capillary melting points apparatus, model 1001, and the given values are uncorrected.

### 4.2. Crystal structure determination

Single-crystal X-ray diffraction data for compounds **9d**, **9h** and **9j** were collected at Oxford Gemini S diffractometer, using monochromatized  $\text{MoK}\alpha$  radiation ( $\lambda = 0.71073 \text{ \AA}$ ). Data reduction and empirical absorption correction were performed with CrysAlisPRO [52]. The crystal structures were solved by direct methods using SHELXS [53] and refined on  $F^2$  by full-matrix least-squares using SHELXL [53]. All non-hydrogen atoms were refined anisotropically. The H atoms bonded to C atoms were placed in geometrically calculated positions and refined using the riding model with  $U_{\text{iso}}$  values constrained to  $1.2U_{\text{eq}}$  or  $1.5U_{\text{eq}}$  of the parent C atoms. The H atoms bonded to N atoms were located in difference Fourier map and refined isotropically. The PLATON [54] software was used to perform geometrical calculation and the Mercury [55] was employed for molecular graphics. Crystallographic details are summarized in Table 4.

**Table 4.** Crystal data and structure refinement parameters.

Compound	<b>9d</b>	<b>9h</b>	<b>9j</b>
Empirical formula	C <sub>21</sub> H <sub>22</sub> FeN <sub>2</sub> O	C <sub>20</sub> H <sub>19</sub> FeN <sub>2</sub> OF	C <sub>20</sub> H <sub>19</sub> FeN <sub>2</sub> OCl
Formula weight	374.26	378.22	394.67
Temperature (K)	293(2)	293(2)	293(2)
Wavelength (Å)	0.71073	0.71073	0.71073
Crystal system	Triclinic	Triclinic	Triclinic
Space group	<i>P</i> -1	<i>P</i> -1	<i>P</i> -1
Unit cell dimensions			
<i>a</i> (Å)	7.1329(4)	7.1095(4)	7.0364(4)
<i>b</i> (Å)	9.2412(4)	9.2090(6)	9.0305(5)
<i>c</i> (Å)	14.3951(6)	13.8244(9)	14.0744(10)
$\alpha$ (°)	104.462(4)	75.131(6)	76.501(5)
$\beta$ (°)	98.613(4)	97.298(5)	88.962(5)
$\gamma$ (°)	103.414(4)	77.021(5)	76.732(4)
<i>V</i> (Å <sup>3</sup> )	871.74(7)	835.90(9)	845.81(9)
<i>Z</i>	2	2	2
<i>D</i> <sub>calc</sub> (Mg/m <sup>3</sup> )	1.426	1.503	1.550
$\mu$ (mm <sup>-1</sup> )	0.876	0.922	1.060
F(000)	392	392	408
Crystal size (mm <sup>3</sup> )	0.51 x 0.26 x 0.09	0.46 x 0.20 x 0.10	0.46 x 0.43 x 0.12
Reflections collected	11450	6391	12871
Independent reflections, <i>R</i> <sub>int</sub>	4061, 0.0249	3769, 0.0240	3983, 0.0264
Data / restraints / parameters	4061 / 0 / 231	3769 / 0 / 230	3983 / 0 / 230
Goodness-of-fit on <i>F</i> <sup>2</sup>	1.050	1.128	1.036
Final <i>R</i> <sub>1</sub> / <i>wR</i> <sub>2</sub> indices [ <i>I</i> > 2σ( <i>I</i> )]	0.0417, 0.1004	0.0419, 0.0929	0.0342, 0.0781
Largest diff. peak and hole (e Å <sup>-3</sup> )	0.619 and -0.344	0.367 and -0.323	0.301 and -0.363

#### 4.3. Electrochemical measurements

Cyclic voltammetry (CV) experiments were performed at ambient temperature in dichloromethane (CH<sub>2</sub>Cl<sub>2</sub>) containing 0.1 M tetrabutylammonium perchlorate (Bu<sub>4</sub>NClO<sub>4</sub>) as the supporting electrolyte. Autolab potentiostat (PGSTAT 302N) and three-electrode cell

were used. The working electrode was the platinum disk ( $d = 2$  mm), and the counter electrode was platinum wire. Ag/AgCl reference electrode (double junction) for nonaqueous systems was used. The working electrode was polished with alumina slurry and rinsed with dichloromethane. The potentials are relative to  $\text{Fc}^+/\text{Fc}$ .

#### 4.4.1 General procedure for the preparation of 3-(arylamino)-1-ferrocenylpropan-1-ones (**1a-k**) and 3-(arylamino)-1-ferrocenylpropan-1-ols (**3a-k**)

The 1,3-amino ketones **1a-k** were prepared following the previously reported procedure [32-38]. A test tube containing a well homogenized mixture of 1-ferrocenylpropanone (240 mg, 1 mmol), the corresponding aniline (2 mmol) and montmorillonite K-10 (100 mg) was placed in the ultrasonic cleaner and irradiated for 1h. Then,  $\text{CH}_2\text{Cl}_2$  (10 ml) was added to the mixture, and the contents were filtered off. The solid residue was washed with water and brine, followed by drying over anhydrous  $\text{Na}_2\text{SO}_4$  overnight. After the evaporation of the solvent, the crude mixture was fractionated by flash chromatography on a  $\text{SiO}_2$  column. The corresponding aniline was eluted with toluene, whereas 3-(arylamino)-1-ferrocenylpropan-1-ones (**1a-k**) were washed from the column by a mixture of hexane and AcOEt 8 : 2 (v/v). The complete excess of the anilines was recovered. The obtained spectral data for 3-(arylamino)-1-ferrocenylpropan-1-ones (**1a-k**) were in complete agreement with literature data [32-39].

The 1,3-amino alcohols **3a-k** were prepared following the previously reported procedure [35-38]. To a stirred solution of the corresponding Mannich base (1 mmol) in MeOH (20 ml) at room temperature, an excess of  $\text{NaBH}_4$  (5 mmol) was added in several portions (up to 190 mg) and the reaction progress was monitored by TLC. After complete reduction (*ca.* 2 h), methanol was distilled off and the residue diluted with water (20 ml). The mixture was extracted with  $\text{CH}_2\text{Cl}_2$  (two 20 ml portions) and the combined organic layers were washed with water and brine, as well as dried over anhydrous  $\text{Na}_2\text{SO}_4$ . After filtering off the drying agent and evaporation of the solvent, the crude product (without purification) was used in the next reaction. The obtained spectral data for 3-(arylamino)-1-ferrocenylpropan-1-ols (**3a-k**) were in complete agreement with literature data [35-38].

#### 4.4.2 General one-pot procedure for the preparation of 1-aryl-4-ferrocenyltetrahydropyrimidin-2(1H)-ones (**9a-k**)

In a test tube, 1 mmol of 1,3-amino alcohol (**3a-k**) was homogenized with 1.5 mmol sodium cyanate ( $\text{NaNCO}$ ), placed in an ultrasonic cleaner and irradiated for 2 hours. Subsequently, 1 ml of glacial acetic acid was added, and the irradiation continued for additional 2 hours. The

reaction mixture was neutralized with NaHCO<sub>3</sub> (litmus paper) and extracted with CH<sub>2</sub>Cl<sub>2</sub> (two 20 ml portions). The combined organic layers were washed with water and brine, as well as dried over anh. Na<sub>2</sub>SO<sub>4</sub>. The solvent was removed by evaporation and the crude product was purified by column chromatography (SiO<sub>2</sub>) to afford pure product **9a-k**.

**4-Ferrocenyl-1-phenyltetrahydropyrimidin-2(1H)-one (9a).**\* Yellow solid; mp 162 °C. R<sub>f</sub> = 0.3 (EtOAc/Hexane, 1:1 (v/v)). Yield 82%. <sup>1</sup>H NMR (200 MHz, CDCl<sub>3</sub>) δ = 7.41 – 7.30 (m, 4H, H-2' and H-3'), 7.23 – 7.14 (m, 1H, 1H, H-4'), 5.22 (br s, 1H, H-3), 4.51 – 4.34 (m, 1H, H-4), 4.31 – 4.16 (overlapped m, 4H, H-2'', H-3'', H-4'' and H-5''), 4.23 (overlapped s, 5H, H-1'''), 3.84 – 3.55 (m, 2H, H-6a and H-6b), 2.34 – 2.13 (m, 1H, H-5a), 2.07 – 1.82 (m, 1H, H-5b). <sup>13</sup>C NMR (50 MHz, CDCl<sub>3</sub>) δ = 154.9 (C-2), 143.4 (C-1'), 128.7 (C-3'), 125.5 (C-2'), 125.4 (C-4'), 90.4 (C-1''), 68.5 (C-1'''), 68.3 (C-3''), 67.9 (C-5''), 66.2 (C-4''), 65.3 (C-2''), 51.0 (C-4), 47.4 (C-6), 31.5 (C-5). \*The assignation for H and C atoms has been done using analogy with examples **9d**, **9h** and **9k** and our previous studies [see references 36, 37]. IR (KBr, cm<sup>-1</sup>) ν = 3424, 1663, 1594, 1575, 753.

**4-Ferrocenyl-1-o-tolyltetrahydropyrimidin-2(1H)-one (9b).**\* Noteworthy, for examples **9b** we have been obtained a mixture of two atropoisomers, therefore, most of the signals in the NMR spectra were double, which was in agreement with our previous studies (for figures of <sup>1</sup>H NMR and <sup>13</sup>C NMR spectra for compound **9b** see ESI) [36, 37]. Yellow solid; mp 167 °C. R<sub>f</sub> = 0.3 (EtOAc/Hexane, 1:1 (v/v)). Yield 70%. <sup>1</sup>H NMR (200 MHz, CDCl<sub>3</sub>) δ = 7.29 – 7.12 (m, 4H, H-3', H-4', H-5' and H-6'), 5.27 (br s, 1H, H-3, diastereoisomer A), 5.22 (br s, 1H, H-3 diastereoisomer B), 4.44 (dd, J = 8.8, 3.5 Hz, 1H, H-3), 4.34 – 4.28 (m, 1H, H-5''), 4.27 – 4.15 (overlapped m, 3H, H-2'', H-3'' and H-4''), 4.23 (overlapped s, 5H, H-1'''), 3.73 – 3.29 (m, 2H, H-6a and H-6b), 2.31 (s, 3H, CH<sub>3</sub>, diastereoisomer A), 2.28 (s, 3H, CH<sub>3</sub>, diastereoisomer B), 2.12 – 1.85 (m, 2H, H-5a and H-5b). <sup>13</sup>C NMR (50 MHz, CDCl<sub>3</sub>)\*\* δ = 154.8 (C-2), 142.0 (C'), 136.1 (C'), 130.9 (C'), 129.2 (C'), 127.9 (C'), 127.6 (C'), 127.3 (C'), 126.8 (C'), 126.1 (C'), 90.7 (C''), 90.4 (C''), 68.6 (C-1'''), 68.3 (C''), 67.7 (C''), 67.7 (C''), 67.4 (C''), 66.2 (C''), 65.5 (C''), 65.2 (C''), 51.2 (C-4), 51.0 (C-4), 47.7 (C-6), 47.3 (C-6), 31.9 (C-5), 31.5 (C-5), 17.8 (CH<sub>3</sub>). \*The assignation for H and C atoms has been done using analogy with example **9d** and our previous studies [see references 36, 37]. \*\*The signals originated from aromatic carbons and substituted Cp ring cannot be assigned based on obtained data. IR (KBr, cm<sup>-1</sup>): ν = 3434, 1660, 1585, 1540, 755.

**4-Ferrocenyl-1-m-tolyltetrahydropyrimidin-2(1H)-one (9c).**\* Yellow solid; mp 154 °C. R<sub>f</sub> = 0.3 (EtOAc/Hexane, 1:1 (v/v)). Yield 81%. <sup>1</sup>H NMR (200 MHz, CDCl<sub>3</sub>) δ = 7.27 – 6.97 (m, 4H, H-2', H-4', H-5' and H-6'), 5.21 (br s, 1H, H-3), 4.39 (dd, J = 8.5, 3.9 Hz, 1H, H-

4), 4.32 – 4.14 (overlapped m, 4H, H-2", H-3", H-4" and H-5"), 4.23 (overlapped s, 5H, H-1"), 3.77 – 3.52 (m, 2H, H-6a and H-6b), 2.35 (s, 3H,  $\underline{\text{CH}}_3$ ), 2.20 (dd,  $J = 13.1, 4.5$  Hz, 1H, H-5a), 1.94 (ddd,  $J = 13.1, 8.8, 4.3$  Hz, 1H, H-5b).  $^{13}\text{C}$  NMR (50 MHz,  $\text{CDCl}_3$ )  $\delta = 155.0$  (C-2), 143.4 (C-1'), 138.6 (C-3'), 128.6 (C-5'), 126.5 (C-2'), 126.4 (C-4'), 122.6 (C-6'), 90.5 (C-1"), 68.5 (C-1""), 68.3 (C-3""), 67.9 (C-5""), 66.2 (C-4""), 65.3 (C-2""), 51.0 (C-4), 47.5 (C-6), 31.5 (C-5), 21.3 ( $\underline{\text{CH}}_3$ ). \*The assignation for H and C atoms has been done using analogy with example **9d** and our previous studies [see references 36, 37]. IR (KBr,  $\text{cm}^{-1}$ ):  $\nu = 3429, 1656, 1608, 1588, 697$ .

**4-Ferrocenyl-1-p-tolyltetrahydropyrimidin-2(1H)-one (9d)**. Yellow solid; mp 191 °C. Rf = 0.3 (EtOAc/Hexane, 1:1 (v/v)). Yield 72%.  $^1\text{H}$  NMR (400 MHz,  $\text{CDCl}_3$ )  $\delta = 7.19$  (q,  $J = 8.2$  Hz, 4H, H-2' and H-3'), 5.13 (br s, 1H, H-3), 4.40 (br d,  $J = 5.1$  Hz, 1H, H-4), 4.30 – 4.16 (overlapped m, 4H, H-2", H-3", H-4" and H-5"), 4.25 (overlapped s, 5H, H-1"), 3.72 (t,  $J = 9.5$  Hz, 1H, H-6a), 3.64 – 3.54 (m, 1H, H-6b), 2.34 (s, 3H,  $\underline{\text{CH}}_3$ ), 2.26 – 2.14 (m, 1H, H-5a), 2.01 – 1.86 (m, 1H, H-5b).  $^{13}\text{C}$  NMR (101 MHz,  $\text{CDCl}_3$ )  $\delta = 155.2$  (C-2), 140.9 (C-1'), 135.4 (C-4'), 129.5 (C-3'), 125.7 (C-2'), 90.5 (C-1"), 68.6 (C-1""), 68.3 (C-3""), 67.9 (C-5""), 66.3 (C-4""), 65.3 (C-2""), 51.1 (C-4), 47.7 (C-6), 31.6 (C-5), 21.0 ( $\underline{\text{CH}}_3$ ). IR (KBr,  $\text{cm}^{-1}$ ):  $\nu = 3422, 1670, 1589, 1565, 692$ . Anal. Calc. for  $\text{C}_{21}\text{H}_{22}\text{FeN}_2\text{O}$ : C, 67.39; H, 5.93; Fe, 14.92; N, 7.49; O, 4.27. Found: C, 67.42; H, 5.90; N, 7.45%.

**4-Ferrocenyl-1-mesityltetrahydropyrimidin-2(1H)-one (9e)**. \* Yellow solid; mp 214 °C. Rf = 0.3 (EtOAc/Hexane, 1:1 (v/v)). Yield 77%.  $^1\text{H}$  NMR (200 MHz,  $\text{CDCl}_3$ )  $\delta = 6.90$  (s, 2H, H-3'), 5.21 (br s, 1H, H-3), 4.42 (dd,  $J = 8.5, 4.0$  Hz, 1H, H-4), 4.33 – 4.27 (m, 1H, H-5"), 4.25 – 4.14 (overlapped m, 3H, H-2", H-3" and H-4"), 4.22 (overlapped s, 5H, H-1"), 3.54 – 3.37 (m, 1H, H-6a), 3.26 (dt,  $J = 12.2, 4.8$  Hz, 1H, H-6b), 2.26 (overlapped s, 6H,  $2 \times \underline{\text{CH}}_3$ ), 2.20 (overlapped s, 3H,  $\underline{\text{CH}}_3$ ), 2.32 – 2.11 (overlapped m, 1H, H-5a), 2.06 – 1.79 (m, 1H, H-5b).  $^{13}\text{C}$  NMR (50 MHz,  $\text{CDCl}_3$ )  $\delta = 154.5$  (C-2), 137.7 (C-1'), 136.9 (C-4'), 135.8 (C-2'), 129.1 (C-3'), 90.5 (C-1"), 68.5 (C-1""), 68.2 (C-3""), 67.7 (C-5""), 66.0 (C-4""), 65.3 (C-2""), 51.0 (C-4), 47.8 (C-6), 31.5 (C-5), 21.8 ( $\underline{\text{CH}}_3$ ), 17.71 ( $2 \times \underline{\text{CH}}_3$ ). \*The assignation for H and C atoms has been done using analogy with example **9d** and our previous studies [see references 36, 37]. IR (KBr,  $\text{cm}^{-1}$ ):  $\nu = 3432, 1656, 1496, 1453, 813$ .

**4-Ferrocenyl-1-(2-fluorophenyl)tetrahydropyrimidin-2(1H)-one (9f)**. \* Yellow solid; mp 179 °C. Rf = 0.4 (EtOAc/Hexane, 1:1 (v/v)). Yield 89%.  $^1\text{H}$  NMR (200 MHz,  $\text{CDCl}_3$ )  $\delta = 7.39$  – 7.05 (m, 4H, H-3', H-4', H-5' and H-6'), 5.59 (br s, 1H, H-3), 4.42 (dd,  $J = 8.1, 4.1$  Hz, 1H, H-4), 4.33 – 4.11 (overlapped m, 4H, H-2", H-3", H-4" and H-5"), 4.22 (overlapped s, 5H, H-1"), 3.72 – 3.43 (m, 2H, H-6a and H-6b), 2.30 – 2.13 (m, 1H, H-5a), 2.04 – 1.83 (m,

1H, H-5b).  $^{13}\text{C}$  NMR (50 MHz,  $\text{CDCl}_3$ )  $\delta$  = 158.2 (d,  $J_{\text{C-F}}$  = 249.3 Hz, C-2'), 154.7 (C-2), 130.5 (d,  $J_{\text{C-F}}$  = 12.2 Hz, C-1'), 129.7 (d,  $J_{\text{C-F}}$  = 1.3 Hz, C-6'), 128.1 (d,  $J_{\text{C-F}}$  = 7.9 Hz, C-4'), 124.2 (d,  $J_{\text{C-F}}$  = 3.7 Hz, C-5'), 116.3 (d,  $J_{\text{C-F}}$  = 20.2 Hz, C-3'), 90.3 (C-1'''), 68.4 (C-1''), 68.1 (C-4''), 67.7 (C-2''), 66.1 (C-3''), 65.3 (C-5''), 50.8 (C-4), 47.2 (C-6), 31.1 (C-5). \*The assignment for H and C atoms has been done using analogy with example **9h** and our previous studies [see references 36, 37]. IR (KBr,  $\text{cm}^{-1}$ ):  $\nu$  = 3424, 1659, 1503, 1488, 753.

**4-Ferrocenyl-1-(3-fluorophenyl)tetrahydropyrimidin-2(1H)-one (9g).**\* Yellow solid; mp 140 °C. Rf = 0.4 (EtOAc/Hexane, 1:1 (v/v)). Yield 93%.  $^1\text{H}$  NMR (200 MHz,  $\text{CDCl}_3$ )  $\delta$  = 7.37 – 7.23 (m, 1H, H-5'), 7.16 – 7.06 (m, 2H, H-2' and H-6'), 6.93 – 6.81 (m, 1H, H-4'), 5.35 (br s, 1H, H-3), 4.47 – 4.33 (m, 1H, H-4), 4.28 – 4.14 (overlapped m, 4H, H-2'', H-3'', H-4'' and H-5''), 4.23 (overlapped s, 5H, H-1'''), 3.81 – 3.55 (m, 2H, H-6a and H-6b), 2.34 – 2.14 (m, 1H, H-5a), 2.05 – 1.84 (m, 1H, H-5a).  $^{13}\text{C}$  NMR (50 MHz,  $\text{CDCl}_3$ )  $\delta$  = 162.6 (d,  $J_{\text{C-F}}$  = 245.3 Hz, C-3'), 154.6 (C-2), 144.9 (d,  $J_{\text{C-F}}$  = 9.9 Hz, C-1'), 129.5 (d,  $J_{\text{C-F}}$  = 9.2 Hz, C-5'), 120.5 (d,  $J_{\text{C-F}}$  = 3.0 Hz, C-6'), 112.6 (d,  $J_{\text{C-F}}$  = 23.6 Hz, C-2'), 112.0 (d,  $J_{\text{C-F}}$  = 21.1 Hz, C-4'), 90.2 (C-1'''), 68.5 (C-1''), 68.3 (C-3''), 67.9 (C-5''), 66.2 (C-4''), 65.3 (C-2''), 50.9 (C-4), 47.1 (C-6), 31.3 (C-5). \*The assignment for H and C atoms has been done using analogy with example **9h** and our previous studies [see references 36, 37]. IR (KBr,  $\text{cm}^{-1}$ ):  $\nu$  = 3419, 1654, 1609, 1590, 693.

**4-Ferrocenyl-1-(4-fluorophenyl)tetrahydropyrimidin-2(1H)-one (9h).** Yellow solid; mp 187 °C. Rf = 0.4 (EtOAc/Hexane, 1:1 (v/v)). Yield 56%.  $^1\text{H}$  NMR (400 MHz,  $\text{CDCl}_3$ )  $\delta$  = 7.33 – 7.28 (m, 2H, H-2'), 7.10 – 7.03 (m, 2H, H-3'), 5.28 (br s, 1H, H-3), 4.42 (dd,  $J$  = 8.6, 4.0 Hz, 1H, H-4), 4.30 – 4.27 (m, 1H, H-2''), 4.27 – 4.23 (overlapped m, 1H, C-4''), 4.23 (overlapped s, 5H, H-1'''), 4.20 – 4.16 (m, 2H, C-3'' and C-5''), 3.71 (ddd,  $J$  = 11.9, 9.9, 3.7 Hz, 1H, H-6a), 3.59 (dt,  $J$  = 11.8, 4.7 Hz, 1H, H-6b), 2.23 (dq,  $J$  = 13.1, 4.0 Hz, 1H, H-5a), 2.00 – 1.91 (m, 1H, H-5b).  $^{13}\text{C}$  NMR (101 MHz,  $\text{CDCl}_3$ )  $\delta$  = 160.4 (d,  $J_{\text{C-F}}$  = 244.8.1 Hz, C-4'), 155.1 (C-2), 139.4 (d,  $J_{\text{C-F}}$  = 3.0 Hz, C-1'), 127.5 (d,  $J_{\text{C-F}}$  = 8.4 Hz, C-2'), 115.6 (d,  $J_{\text{C-F}}$  = 22.5 Hz, C-3'), 90.3 (C-1'''), 68.6 (C-1''), 68.4 (C-3''), 68.0 (C-5''), 66.3 (C-4''), 65.3 (C-2''), 51.1 (C-4), 47.7 (C-6), 31.5 (C-5). IR (KBr,  $\text{cm}^{-1}$ ):  $\nu$  = 3418, 1664, 1508, 1483, 822. Anal. Calc. for  $\text{C}_{20}\text{H}_{19}\text{FFeN}_2\text{O}$ : C, 63.51; H, 5.06; F, 5.02; Fe, 14.76; N, 7.41; O, 4.23. Found: C, 63.55; H, 5.01; N, 7.38%.

**1-(2-Chlorophenyl)-4-ferrocenyltetrahydropyrimidin-2(1H)-one (9i).**\* Yellow oil. Rf = 0.2 (EtOAc/Hexane, 1:1 (v/v)). Yield 60%.  $^1\text{H}$  NMR (200 MHz,  $\text{CDCl}_3$ )  $\delta$  = 7.46 (dd,  $J$  = 6.7, 2.3 Hz, 1H, H-5'), 7.38 – 7.19 (m, 3H, H-2', H-4' and H-6'), 5.37 (br d,  $J$  = 9.2 Hz, 1H, H-3), 4.42 (dd,  $J$  = 9.9, 6.0 Hz, 1H, H-4), 4.37 – 4.26 (m, 1H, H-5''), 4.26 – 4.13 (overlapped

m, 3H, H-2", H-3" and H-4"), 4.23 (overlapped s, 5H, H-1""), 3.84 – 3.28 (m, 2H, H-6a and H-6b), 2.35 – 1.88 (m, 2H, H-5a and H-5b).  $^{13}\text{C}$  NMR (50 MHz,  $\text{CDCl}_3$ )  $\delta = 154.6$  (C-2), 140.4 (C'), 133.1 (C'), 130.3 (C'), (C'), 128.5 (C'), 127.7 (C'), 90.4 (C-1"), 68.5 (C-1""), 68.2 (C-3"), 67.8 (C-5"), 66.2 (C-4"), 65.4 (C-2"), 50.1 (C-4), 47.2 (C-6), 31.3 (C-5). \*The assignation for H and C atoms has been done using analogy with example **9k** and our previous studies [see references 36, 37]. \*\*The signals originated from aromatic carbons cannot be assigned based on obtained data. IR (KBr,  $\text{cm}^{-1}$ ):  $\nu = 3438, 1646, 1495, 1448, 755$ .

**1-(3-Chlorophenyl)-4-ferrocenyltetrahydropyrimidin-2(1H)-one (9j).**\* Yellow solid; mp 169 °C. Rf = 0.4 (EtOAc/Hexane, 1:1 (v/v)). Yield 83%.  $^1\text{H}$  NMR (200 MHz,  $\text{CDCl}_3$ )  $\delta = 7.35$  (s, 1H, H-2'), 7.28 – 7.23 (m, 2H, H-4' and H-6'), 7.19 – 7.12 (m, 1H, H-5'), 5.43 (br s, 1H, H-3), 4.40 (dd,  $J = 8.7, 3.7$  Hz, 1H, H-4), 4.29 – 4.16 (overlapped m, 4H, H-2", H-3", H-4" and H-5"), 4.23 (overlapped s, 5H, H-1""), 3.78 – 3.54 (m, 2H, H-6a and H-6b), 2.29 – 2.15 (m, 1H, H-5a), 2.09 – 1.84 (m, 1H, H-5b).  $^{13}\text{C}$  NMR (50 MHz,  $\text{CDCl}_3$ )  $\delta = 154.6$  (C-2), 144.5 (C-1'), 134.0 (C-3'), 129.5 (C-6'), 125.5 (C-2'), 125.4 (C-5'), 123.5 (C-4'), 90.2 (C-1"), 68.5 (C-1""), 68.3 (C-3"), 67.9 (C-5"), 66.2 (C-4"), 65.3 (C-2"), 50.9 (C-4), 47.1 (C-6), 31.2 (C-5). \*The assignation for H and C atoms has been done using analogy with example **9k** and our previous studies [see references 36, 37]. IR (KBr,  $\text{cm}^{-1}$ ):  $\nu = 3424, 1667, 1590, 1570, 755$ . Anal. Calc. for  $\text{C}_{20}\text{H}_{19}\text{ClFeN}_2\text{O}$ : C, 60.86; H, 4.85; Cl, 8.98; Fe, 14.15; N, 7.10; O, 4.05. Found: C, 60.90; H, 4.90; N, 7.15%.

**1-(4-Chlorophenyl)-4-ferrocenyltetrahydropyrimidin-2(1H)-one (9k).** Yellow solid; mp 183 °C. Rf = 0.4 (EtOAc/Hexane, 1:1 (v/v)). Yield 76%.  $^1\text{H}$  NMR (400 MHz,  $\text{CDCl}_3$ )  $\delta = 7.38 - 7.21$  (m, 4H, H-2', H-3', H-5' and H-6'), 5.24 (br s, 1H, H-3), 4.44 (br s, 1H, H-4), 4.32 – 4.15 (overlapped m, 4H, H-2", H-3", H-4" and H-5"), 4.23 (overlapped s, 5H, H-1""), 3.82 – 3.56 (m, 2H, H-6a and H-6b), 2.22 (br d,  $J = 10.7$  Hz, 1H, H-5a), 2.02 – 1.85 (m, 1H, H-5b).  $^{13}\text{C}$  NMR (101 MHz,  $\text{CDCl}_3$ )  $\delta = 141.7$  (C-2), 130.8 (C-1'), 128.7 (C-4'), 126.7 (C-2'), 120.8 (C-3'), 90.1 (C-1"), 68.5 (C-1""), 68.3 (C-3") 67.9 (C-5"), 66.2 (C-4"), 65.1 (C-2"), 50.9 (C-4), 47.3 (C-6), 31.3 (C-5). IR (KBr,  $\text{cm}^{-1}$ ):  $\nu = 3420, 1665, 1610, 1568, 750$ .

## Acknowledgement

This work was supported by the Ministry of Education, Science and Technological development of the Republic of Serbia (Agreement No. 451-03-68/2020-14/200122).

## Supporting Information

X-ray crystallographic data in CIF format and copies of IR and NMR ( $^1\text{H}$  NMR and  $^{13}\text{C}$  NMR) spectra.

## Appendix A. Supplementary data

Crystallographic data for structural analysis have been deposited with the Cambridge Crystallographic Data Centre, CCDC No. 2000137-2000139. These data can be obtained free of charge via [www.ccdc.cam.ac.uk](http://www.ccdc.cam.ac.uk).

## References

- [1] S. K. Kashawa, V. Kashawa, P. Mishra, N. K. Jain, J. P. Stables, *Eur. J. Med. Chem.* 44 (2009) 4335 - 4343.
- [2] (a) S. A. Khan, N. Singh, K. Saleem, *Eur. J. Med. Chem.* 43 (2008) 2272 - 2277; (b) N. Selvakumar, G. G. Rajulu, K. C. S. Reddy, B. C. Chary, P. K. Kumar, T. Madhavi, K. Praveena, K. H. P. Reddy, M. Takhi, A. Mallick, P. V. S. Amarnath, S. Kandepu, J. Iqbal, *Bioorg. Med. Chem. Lett.* 18 (2008) 856 - 860; (c) T. Kaneko, W. McMillen, M. K. Lynch, *Bioorg. Med. Chem. Lett.* 17 (2007) 5013 - 5018; (d) S. Hudson, M. Kiankarimi, M. W. Rowbottom, T. D. Vickers, D. Wu, J. Pontillo, B. Ching, W. Dwight, V. S. Goodfellow, D. Schwarz, C. E. Heise, A. Madan, J. Wen, W. Ban, H. Wang, W. S. Wade, *Bioorg. Med. Chem. Lett.* 16 (2006) 4922 - 4930.
- [3] (a) T. C. McMorris, R. Chimmani, K. Alisala, M. D. Staake, G. Banda, M. J. Kelner, *J. Med. Chem.* 53 (2010) 1109 - 1116; (b) R. Kakadiya, H. Dong, A. Kumar, D. Narsinh, X. Zhang, T. C. Chou, T. C. Lee, A. Shah, T. L. Su, *Bioorg. Med. Chem.* 18 (2010) 2285 - 2299; (c) H. Q. Li, T. T. Zhu, T. Yan, Y. Luo, H. L. Zhu, *Eur. J. Med. Chem.* 44 (2009) 453 - 459.
- [4] (a) M. Fernandez, J. Caballero, *Bioorg. Med. Chem.* 16 (2006) 280 - 284; (b) C. Zhao, H. L. Sham, M. Sun, V. S. Stoll, K. D. Stewart, S. Lin, H. Mo, S. Vasavanonda, A. Saldivar, C. Park, E. J. McDonald, K. C. Marsh, L. L. Klein, D. J. Kempf, D. W. Norbeck, *Bioorg. Med. Chem. Lett.* 15 (2005) 5499 - 5503; (c) P. P. Huang, J. T. Randolph, L. L. Klein, S. Vasavanonda, T. Dekhtyar, V. S. Stol, D. J. Kempf, *Bioorg. Med. Chem. Lett.* 14 (2004) 4075 - 4078.

- [5] (a) M. Berlin, Y. J. Lee, C.W. Boyce, Y. Wang, R. Aslanian, K. D. McCormick, S. Sorota, S. M. Williams, R. E. West, W. Korfmacher, *Bioorg. Med. Chem. Lett.* 20 (2010) 2359 - 2364; (b) R. J. Perner, S. Domenico, J. R. Koenig, A. Gomtsyan, E. K. Bayburt, R. G. Schmidt, I. Drizin, G. Z. Zheng, S.C. Turner, T. Jinkerson, B. S. Brown, R.G. Keddy, K. Lukin, H.A. McDonald, P. Honore, J. Mikusa, K. C. Marsh, J. M. Wetter, K. George, M. F. Jarvis, C. R. Faltynek, C. H. Lee, *J. Med. Chem.* 50 (2007) 3651 - 3660; (c) M. W. Rowbottom, T. D. Vickers, B. Dyck, J. Tamiya, M. Zhang, L. Zhao, J. Grey, D. Provencal, D. Schwarz, C. E. Heise, M. Mistry, A. Fisher, T. Dong, T. Hu, J. Saunders, V. S. Goodfellowa, *Bioorg. Med. Chem. Lett.* 15 (2005) 3439 - 3445.
- [6] M. Radić Stojković, S. Marzi, Lj. Glavaš-Obrovac, I. Piantanida, *Eur. J. Med. Chem.* 45 (2010) 3281 - 3292.
- [7] E.L. Luzina, A.V. Popov, *Eur. J. Med. Chem.* 45 (2010) 5507 - 5512.
- [8] R.H. Tale, A.H. Rodge, G.D. Hatnapure, A.P. Keche, *Bioorg. Med. Chem. Lett.* 21 (2011) 4648 - 4651.
- [9] M. Kurihara, A. S. S. Rouf, H. Kansui, H. Kagechika, H. Okuda, N. Miyata, *Bioorg. Med. Chem. Lett.* 14 (2004) 4131 - 4134.
- [10] (a) P. Babczinski, G. Sandmann, R. R. Schmidt, K. Shiokawa, K. Yasui, *Pestic. Biochem. Physiol.* 52 (1995) 33 - 44; (b) P. Babczinski, M. Blunck, G. Sandmann, K. Shiokawa, K. Yasui, *Pestic. Biochem. Physiol.* 52 (1995) 45 - 59.
- [11] T. J. Kealy, P. L. Pauson, *Nature* 168 (1951) 1039 - 1040.
- [12] (a) A. Togni, T. Hayashi, *Ferrocenes: Homogeneous Catalysis, Organic Synthesis, Materials Science*, Wiley-VCH, Weinheim, (1995); (b) P. Štěonička, *Ferrocenes: Ligands, Materials and Biomolecules*, John Wiley & Sons, Ltd., Chichester, (2008); (c) S. Kaur, M. Kaur, P. Kaur, K. Clays, K. Singh, *Coordin. Chem. Rev.* 343 (2017) 185 - 219.
- [13] M. Koketsu, K. Tanaka, Y. Takenaka, C. D. Kwong, H. Ishihara, *Eur. J. Pharm. Sci.* 15 (2002) 307 - 310.
- [14] C. Biot, N. Francois, L. Maciejewski, J. Brocard, D. Poulain, *Bioorg. Med. Chem. Lett.* 10 (2000) 839 - 841.
- [15] T. Itoh, S. Shirakami, N. Ishida, Y. Yamashita, T. Yoshida, H.S. Kim, Y. Wataya, *Bioorg. Med. Chem. Lett.* 10 (2000) 1657 - 1659.

- [16] C. Baldoli, S. Maiorana, E. Licandro, G. Zinzalla, D. Perdicchia, *Org. Lett.* 4 (2002) 4341 - 4344.
- [17] J. Cuzick, T. Powles, U. Veronesi, J. Forbes, R. Edwards, S. Ashley, P. Boyle, *The Lancet.* 361 (2003) 296 - 300.
- [18] A. Vessieres, S. Top, W. Beck, E. Hillarda, G. Jaouen, *Dalton Trans.* (2006) 529 - 541.
- [19] A. Vessieres, S. Top, P. Pigeon, E. Hillard, L. Boubeker, D. Spera, G. Jaouen, *J. Med. Chem.* 48 (2005) 3937 - 3940.
- [20] E. Hillard, A. Vessieres, F. Le Bideau, D. Plazuk, D. Spera, M. Huch, G. Jaouen, *ChemMedChem.* 1 (2006) 551 - 559.
- [21] (a) K. Kowalski, *Coordin. Chem. Rev.* 366 (2018) 91 - 108; (b) F. A. Larik, A. Saeed, T. A. Fattah, U. Muqadar, P. A. Channar, *Appl. Organometal. Chem.* 31 (2017) 3664; (c) M. Parta, G. Gasser, *Nat. Rev. Chem.* 1 (2017) article number 0066; (d) M. F. R. Fouda, M. M. Abd-Elzaher, R. A. Abdelsamaia, A. A. Labib, *Appl. Organometal. Chem.* 21 (2007) 613 - 625.
- [22] D. Ilić, I. Damljanović, D. Stevanović, M. Vukićević, N. Radulović, V. Kahlenberg, G. Laus, R. D. Vukićević, *Polyhedron* 29 (2010) 1863 – 1869.
- [23] D. Ilić, I. Damljanović, D. Stevanović, M. Vukićević, P. Blagojević, N. Radulović, R. D. Vukićević, *CHEMISTRY & BIODIVERSITY* 9 (2012) 2236 – 2253.
- [24] A. Pejović, I. Damljanović, D. Stevanović, D. Ilić, M. Vukićević, G. A. Bogdanović, R. D. Vukićević, *Tetrahedron Lett.* 54 (2013) 4776 – 4780.
- [25] A. Pejović, I. Damljanović, D. Stevanović, M. Vukićević, S. B. Novaković, G. A. Bogdanović, N. Radulović, R. D. Vukićević, *Polyhedron* 31 (2012) 789 - 795.
- [26] A. Pejović, I. Damljanović, D. Stevanović, A. Minić, J. Jovanović, V. Mihailović, J. Katanić, G. A. Bogdanović, *J. Organomet. Chem.* 846 (2017) 6 - 17.
- [27] A. Pejović, A. Minić, J. Bugarinović, M. Pešić, I. Damljanović, D. Stevanović, V. Mihailović, J. Katanić, G. A. Bogdanović, *Polyhedron* 155 (2018) 382 - 389.
- [28] A. Pejović, A. Minić, J. Jovanović, M. Pešić, D. Ilić Komatina, I. Damljanović, D. Stevanović, V. Mihailović, J. Katanić, G. A. Bogdanović, *J. Organomet. Chem.* 869 (2018) 1 - 10.

- [29] J. P. Bugarinović, M. S. Pešić, A. Minić, J. Katanić, D. Ilić-Komatina, A. Pejović, V. Mihailović, D. Stevanović, B. Nastasijević, I. Damljanović, *J. Inorg. Biochem.* 189 (2018) 134 - 142.
- [30] M. Pešić, J. Bugarinović, A. Minić, S. Novaković, G. Bogdanović, A. Todosijević, D. Stevanović, I. Damljanović, *Bioelectrochemistry* 132 (2020) 107412 - 107419.
- [31] A. Minić, T. Van de Walle, K. Van Hecke, J. Combrinck, P. J. Smith, K. Chibale, M. D'hooghe, *Eur. J. Med. Chem.* 187 (2020) 111963 - 111977.
- [32] I. Damljanović, D. Stevanović, A. Pejović, M. Vukićević, S. B. Novaković, G. A. Bogdanović, T. Mihajilov-Krstev, N. Radulović, R. D. Vukićević, *J. Organomet. Chem.* 696 (2011) 3703 - 3713.
- [33] A. Pejović, D. Stevanović, I. Damljanović, M. Vukićević, S. B. Novaković, G. A. Bogdanović, T. Mihajilov-Krstev, N. Radulović, R. D. Vukićević, *Helv. Chim. Acta* 95 (2012) 1425 - 1441.
- [34] A. Minić, J. P. Jovanović, G. A. Bogdanović, A. Pejović, N. Radulović, I. Damljanović, D. Stevanović, *Polyhedron* 141 (2018) 343 - 351.
- [35] A. Minić, J. Bugarinović, A. Pejović, D. Ilić-Komatina, G. A. Bogdanović, I. Damljanović, D. Stevanović, *Tetrahedron Lett.* 59 (2018) 3499 - 3502.
- [36] A. Minić, D. Stevanović, I. Damljanović, A. Pejović, M. Vukićević, G. A. Bogdanović, N. S. Radulović, R. D. Vukićević, *RSC Adv.* 5 (2015) 24915 - 24919.
- [37] A. Minić, S. B. Novaković, G. A. Bogdanović, J. P. Bugarinović, M. S. Pešić, A. Todosijević, D. Ilić Komatina, I. Damljanović, D. Stevanović, *Polyhedron* 177 (2020) 114316 - 114325.
- [38] A. Minić, D. Stevanović, M. Vukićević, G. A. Bogdanović, M. D'hooghe, N. S. Radulović, R. D. Vukićević, *Tetrahedron* 73 (2017) 6268 - 6274.
- [39] A. Minić, J. Bugarinović, M. Pešić, D. Ilić Komatina, *UNIVERSITY THOUGHT - Publication in Natural Sciences*, 9 (2019) 38 - 44.
- [40] (a) A. F. Hegarty, L. J. Drennan, *Comprehensive Organic Functional Group Transformations*, Pergamon, Oxford, (2003); (b) O. V. Denisko, *Comprehensive Organic Functional Group Transformations II*, Elsevier, Amsterdam, (2004).

- [41] (a) P. Gayathri, V. Pande, R. Sivakumar, S. P. Gupta, *Bioorg. Med. Chem.* 9 (2001) 3059 - 3063; (b) J. H. Saunders, R. J. Slocombe, *Chem. Rev.* 43 (1948) 203 - 218; (c) S. Ozaki, *Chem. Rev.* 72 (1972) 457 - 496.
- [42] (a) A. Basha, *Tetrahedron Lett.* 29 (1988) 2525 - 2526; (b) R. A. Stachell, D. P. N. Stachell, *Chem. Soc. Rev.* 4 (1975) 231 - 250.
- [43] L. De Luca, A. Porcheddu, G. Giacomelli, I. Murgia, *SYNLETT* 16 (2010) 2439–2442.
- [44] X. Min, J. Liu, Y. Dong, M. Hussain, *Synthesis* 50 (2018) 341–348.
- [45] (a) A. Williams, W. P. Jencks, *J. Chem. Soc., Perkin Trans. 2* (1974) 1753-1759; (b) A. Williams, W. A. Jencks, *J. Chem. Soc., Perkin Trans. 2* (1974) 1760-1768.
- [46] C. Bleiholder, F. Rominger, R. Gleiter, *Organometallics*. 28 (2009) 1014 - 1017.
- [47] G. Bogdanović, S. Novaković, *CrystEngComm* 13 (2011) 6930–6932.
- [48] M. A. Spackman, D. Jayatilaka, *CrystEngComm* 11 (2009) 19–32.
- [49] G. Elmas, A. Okumus, L. Y. Koç, H. Soltanzade, Z. Kılıç, T. Hõkelek, H. Dal, L. Açık, Z. Üstündag, D. DüNDAR, M. Yavuz, *Eur. J. Med. Chem.* 87 (2014) 662 - 676.
- [50] R. Chopra, C. de Kock, P. Smith, K. Chibale, K. Singh, *Eur. J. Med. Chem.* 100 (2015) 1 - 9.
- [51] A. J. Bard, L. R. Faulkner, *Electrochemical Methods: Fundamentals and Applications - 2nd ed.*, John Wiley and Sons, Inc, Hoboken (2001).
- [52] Rigaku Oxford Diffraction, CrysAlisPro Software system, Rigaku Corporation, Oxford, UK, 2015.
- [53] G.M. Sheldrick, *Acta Crystallogr. C* 71 (2015) 3–8.
- [54] A.L. Spek, *J. Appl. Crystallogr.* 36 (2003) 7–13.
- [55] C.F. Macrae, P.R. Edgington, P. McCabe, E. Pidcock, G.P. Shields, R. Taylor, M. Towler, J.V. Streek, *J Appl. Crystallogr.* 39 (2006) 453–457.

## Schemes and figure captions

**Scheme 1.** Synthesis of Fc-containing compounds starting from Mannich bases. Reagents and conditions: *i*) PhNCO, ultrasound irradiation for 1h; *ii*) NaBH<sub>4</sub>, MeOH, stirring for 2h; *iii*) PhNCS, ultrasound irradiation (1-7 h), then AcOH, ultrasound irradiation, 1 h; *iv*) PhNCO, ultrasound irradiation, 1 h, and then AcOH, ultrasound irradiation, 1 h; *v*) AcOH, ultrasound irradiation, 2 h; *vi*) DDQ, toluene, reflux for 2 h.

**Scheme 2.** A synthetic strategy to 1-aryl-4-ferrocenyltetrahydropyrimidin-2(1*H*)-ones (**9a-k**)

**Scheme 3.** An overview of newly Fc-containing tetrahydropyrimidin-2(1*H*)-ones **9a-k**

**Scheme 4.** Plausible schematic mechanism for the synthesis of titled compounds **9a-k**

**Figure 1.** The IR spectra (800-3600cm<sup>-1</sup>) for compound **9a**

**Figure 2.** Labeled carbons atoms for NMR characterization

**Figure 3.** The molecular structure with the atom-labelling scheme: (a) **9d**, (b) **9h** and (c) **9j**.

Displacement ellipsoids are drawn at the 30% probability level.

**Figure 4.** (a) Overlay of **9d**, **9h** and **9j** (blue, green and red, respectively) based on the atoms of Cp1 ring. Overlay of **9d** (blue) and the N2-substituted derivative [36] (yellow); atom-labelling scheme in (b) corresponds only to the yellow colored molecule, atom-labelling of **9d** is as in (a) where this molecule is presented in the same orientation. H atoms are excluded for clarity.

**Figure 5.** Double chain of **9d** molecules formed by N2–H...O1 hydrogen bond, Fc...Fc pairing and C17–H...π interaction. Equivalent chains for **9h** and **9j** are presented in Figure S2 and Figure S3 (see *ESI*).

**Figure 6.** Cyclic voltammograms at the platinum disk (d = 2 mm) by a 0.1 V s<sup>-1</sup> scan rate in 0.1 M dichloromethane solution of Bu<sub>4</sub>NClO<sub>4</sub>: (a) electrolyte, (b) 1 mM solution of 4-ferrocenyl-1-phenyltetrahydropyrimidin-2(1*H*)-one (**9a**) (c) ferrocene.

**Figure 7.** Cyclic voltammograms of 1 mM solution of 4-ferrocenyl-1-phenyltetrahydropyrimidin-2(1*H*)-one (**9a**) at the platinum disk (d = 2 mm) in 0.1 M dichloromethane solution of Bu<sub>4</sub>NClO<sub>4</sub> on a different scan rates: a) 0.01 V s<sup>-1</sup> b) 0.1 V s<sup>-1</sup> c) 0.3 V s<sup>-1</sup> d) 0.5 V s<sup>-1</sup>

**Figure 8.** Anodic and cathodic peak currents of product **9a** obtained at different scan rates at the platinum disk (d = 2 mm) in 0.1 M dichloromethane solution of Bu<sub>4</sub>NClO<sub>4</sub>.

## Highlights

- An efficient one-pot synthetic procedure for the preparation of 1-aryl-4-ferrocenyltetrahydropyrimidin-2(1*H*)-ones has been developed
- Eleven novel ferrocene-containing tetrahydropyrimidin-2(1*H*)-ones were synthesized in good to high yields (up to 93%)
- All products have been isolated in high purity >95% and a detailed spectroscopic characterization has been provided
- A detailed single-crystal X-ray diffraction analysis was successfully performed on three examples
- Electrochemical behavior of newly synthesized has been evaluated by the usage of cyclic voltammetry

**Declaration of interests**

The authors declare that they have no known competing financial interests or personal relationships that could have appeared to influence the work reported in this paper.

The authors declare the following financial interests/personal relationships which may be considered as potential competing interests:

Journal Pre-proof